Precambrian Research 405 (2024) 107366

Contents lists available at ScienceDirect

Precambrian Research

journal homepage: www.elsevier.com/locate/precamres

Pan-African granitic magmatism of the Kaoko Belt: Tectonic perspective from its South American connection and insights into the crustal architecture of SW Gondwana

Mathias Hueck [a,b,*], Miguel A.S. Basei [b], Hartwig Frimmel [c], Lucas M. Lino [b], Vinicius X. Corrêa [b], Lucas R. Tesser [b], Mario C. Campos Neto [b], Carlos E. Ganade [d]

[a] Institute for Geology, Mineralogy and Geophysics, Bochum, Germany
[b] Instituto de Geociências, Universidade de São Paulo, Brazil
[c] Institute of Geography and Geology, University of Würzburg, Germany
[d] Center of Applied Geosciences, Geological Survey of Brazil, Rio de Janeiro, Brazil

ARTICLE INFO

Keywords:
Whole-rock isotope geochemistry
isotope geochemistry, U-Pb zircon
Magmatic sources

ABSTRACT

The Kaoko Belt in northwestern Namibia formed during the assembly of Gondwana in the Neoproterozoic to Cambrian Pan-African orogenic cycle. The belt has a complex tectonic architecture, in which a variety of basement units and metasedimentary associations became juxtaposed along shear zones and experienced widespread intrusive magmatism, generally confined to its western domain. We present a large new dataset of whole-rock geochemical and isotope data, as well as U-Pb zircon ages, encompassing a wide variety of granitoids and subordinate basic rocks across the Kaoko Belt. This is complemented by whole-rock isotope analyses from various basement and metasedimentary units and by a compilation of data from the literature. The new dataset strengthens previous models that correlate the granitoids in the Kaoko Belt to the coeval Florianópolis Batholith in the South American Dom Feliciano Belt, which we use to shed new light on the tectonic organization and evolution of the Pan-African orogenic cycle in the Neoproterozoic. The similarities in the compositional range of granitoids from both sub-domains of the Western Kaoko Belt, namely the Orogen Core and the Coastal Terrane, suggest that the entire zone comprises a heterogeneous but comparable and consistently diverse association of rocks. The comparison to South America underscores that, while the granitoids have "crust-like" isotopic signatures, these are in sharp contrast with those of the mostly Archean to Paleoproterozoic basement rocks of both the Kaoko and Dom Felicano belts. This suggests that the magmatic sources of the intrusive magmatism of the Kaoko Belt are likely a mixture of autochthonous crustal melting with an important mantle-derived input at some point after the Paleoproterozoic. This input was probably driven by accretionary orogeny and/or rifting that took place in the Tonian, Ediacaran, or both. The presence of more juvenile associations in the western domain of the Kaoko Belt may indicate an isotopic boundary within the belt that mirrors the tectonic configuration of the Dom Feliciano Belt in South America. This isotopic border, which would correspond to the Puros Shear Zone, could have acted as a terrane boundary from the earliest stages of the tectonic evolution of the Kaoko Belt.

1. Introduction

The near-ubiquitous presence of intermediate to silicic intrusive igneous rocks (granitoids sensu lato) in all types of orogenic belts means that understanding their petrogenesis is an invaluable asset for recovering crustal growth/recycling mechanisms and reconstructing tectonic processes (Brown, 2007; Saint Blanquat et al., 2011; Annen et al., 2015; Moyen et al., 2021; Jacob et al., 2021). Especially in the case of syn- to post-collisional systems, in which the contribution of magma from the partial melting of crustal material is of enormous importance (*e.g.,* Miller et al., 2003; Cawood et al., 2013; Jacob et al., 2021), these rocks can also constitute tracers of magmatic sources within the continental crust and act as windows to the tectonic architecture of their host system by combining tools such as whole-rock geochemistry, isotope studies, and (inherited) zircon geochronology (Villaros et al., 2012; Gaschnig et al., 2013; Laurent et al., 2014; Moyen et al., 2017; Gao et al., 2023).

* Corresponding author.
E-mail address: mathiashueck@gmail.com (M. Hueck).

https://doi.org/10.1016/j.precamres.2024.107366
Received 7 November 2023; Received in revised form 5 March 2024; Accepted 11 March 2024
Available online 16 March 2024

The joint use of bulk-rock geochemistry, isotope geochemistry and U-Pb-Hf isotope ratios in zircon has proven to be effective in recognizing variations in the crustal sources of the widespread granitic magmatism in the Neoproterozoic Pan-African Dom Feliciano Belt in South America (Florisbal et al., 2012a; Hueck et al., 2016, 2020a; Lara et al., 2020, 2021). The Kaoko Belt in northwestern Namibia, the tectonic counterpart of the Dom Feliciano Belt across the South Atlantic (Frimmel et al., 2011; Oyhantçabal et al., 2011; Konopásek et al., 2016, 2018; Basei et al., 2018; Will et al., 2020; Silva Lara et al., 2022), is also characterized by abundant and widespread Neoproterozoic magmatic rocks, especially in its western domains (Masberg et al., 2005; Konopásek et al., 2008; Jung et al., 2009; Janoušek et al., 2010, 2023). However, whereas individual magmatic associations have been the focus of detailed petrogenetic considerations, the magmatic record of the Kaoko Belt as a whole has not been studied so far, largely due to a lack of a comprehensive database. Moreover, as the Kaoko Belt has a complex internal architecture with a remarkable variety of basement fragments, this kind of analyses has the potential of providing valuable insights into the tectonic organization and evolution of the orogen.

In order to address the above, this paper presents a large new dataset of geochemical data (major and trace elements, as well as Rb-Sr and Sm-Nd isotopes) and zircon U-Pb ages of Neoproterozoic granitoids and subordinate associated basic-intermediate rocks from the Kaoko Belt. This is complemented by data from the literature and by whole-rock isotope analyses from a series of basement and metasedimentary samples from the various domains of the belt. Based on the compiled dataset, and considering its connections to comparable units in South America, we discuss the possible magmatic sources of the magmatism, as well as the implications for the tectonic evolution and crustal architecture of southwestern Gondwana during the Pan-African orogenic cycle.

2. Geological setting

The assembly of southwestern Gondwana during the Neoproterozoic Pan-African orogenic cycle led to the formation of a system of orogenic belts surrounding cratonic nuclei that characterize the basement geology of the South Atlantic coasts of Africa and South America. The southernmost belts in this system are the Dom Feliciano Belt in southeastern South America (*e.g.,* Hueck et al., 2018 and references therein), and the Saldania, Gariep, Damara and Kaoko belts in southwestern Africa (Frimmel, 2018; Goscombe et al., 2018 and references therein). These systems were formed during the tectonic interaction of the Congo, Kalahari, and Rio de la Plata cratons, along with several smaller crustal fragments (Frimmel et al., 2011; Basei et al., 2018; Konopásek et al., 2018, 2020; Hueck et al., 2022). Credible correlations between the western terranes of the Kaoko Belt and the easternmost units of the Dom Feliciano Belt are among the best direct links between the geology on both sides of the South Atlantic (Frimmel et al., 2011; Oyhantçabal et al., 2011; Konopásek et al., 2016, 2018; Basei et al., 2018; Will et al., 2020; Silva Lara et al., 2022), and are thus particularly important in the reconstruction of the paleogeography and tectonic models of southwest Gondwana. In addition, a series of Archean to Proterozoic basement fragments in the southern South American Platform may have been parts of the Angola Block (Congo Craton) prior to the Pan-African orogenic cycle (Hueck et al., 2022).

2.1. The Kaoko Belt

The Kaoko Belt follows the South Atlantic coast from southern Angola to central Namibia for over 400 km. It mostly comprises an association of Neoproterozoic metasupracrustal rocks (Damara Supergroup) with exposures of Archean and Proterozoic basement rocks, along with widespread Neoproterozoic granitic intrusions. The architecture of the Kaoko Belt is divided into four main segments (Goscombe et al., 2003a, 2017, 2018; Goscombe & Gray, 2008; Ulrich et al., 2011; Fig. 1), from east to west: the Eastern Kaoko Zone (foreland); the Central Kaoko Zone (orogenic escape Zone); and the Western Kaoko Zone, which is further divided into the Orogen Core to the east and the Coastal Terrane to the west. Each domain is separated from each other by major structural lineaments and shear zones (Goscombe & Gray, 2008; Foster et al., 2009; Oriolo et al., 2018).

The Eastern Kaoko Zone corresponds to a foreland fold-and-thrust belt overlying basement rocks, the largest of which is the Paleoproterozoic Kamanjab Inlier (*e.g.,* Kleinhanns et al., 2015), which are commonly ascribed to the Angola Block, and, consequently, the Congo Craton (Jelsma et al., 2018). An alternative interpretation of the Angola Block having drifted off the Kalahari Craton in the early Neoproterozoic has also been speculated upon (Frimmel et al., 2011). The sedimentary cover comprises predominantly carbonatic rocks of the Otavi Group and includes two diamictite units that record the Stuartian and Marinoan glaciations, respectively, covered by molasse sediments of the Ediacaran Mulden Group (Hoffman et al., 1998, 2021; Konopásek et al., 2017). The sequence was exposed to sub-greenschist facies temperatures and records east-verging folds truncated by a system of brittle west-dipping thrust faults that culminates in the Sesfontein Thrust at the western margin of the zone (Goscombe & Gray, 2008; Oriolo et al., 2018).

To the west of the Sesfontein Thrust, the Central Kaoko Zone is dominated by a medium-grade metasedimentary sequence in complex association with basement inliers. Basement rocks are diverse and include relatively confined Archean associations to the south, as well as a predominantly Paleoproterozoic association with subordinately Mesoproterozoic intrusive bodies, grouped together as the large Epupa Complex to the north and extending into southern Angola (Seth et al., 1998; Franz et al., 1999; Kröner et al., 2004, 2010, 2015; Jung et al., 2012; Kröner & Rojas-Agramonte, 2017). The metasedimentary association includes mainly metaturbidites and records a Barrovian metamorphic sequence from greenschist to upper-amphibolite facies, stacked by E-verging nappes that become tighter and steeper to the west, culminating in the Puros Shear Zone (Goscombe et al., 2003a, b, 2005a; Will et al., 2004; Goscombe & Gray, 2008; Seth et al., 2008; Jung et al., 2014). This shear zone is the clearest structural lineament of the Kaoko Belt, and corresponds to a mylonitic belt, up to 5 km wide, with predominantly sinistral strike-slip and inverse kinematics, developed mainly under amphibolite-facies conditions (Konopásek et al., 2005; Goscombe & Gray, 2008; Ulrich et al., 2011; Oriolo et al., 2018).

The eastern portion of the Western Kaoko Zone, also known as the Orogenic Core, encompasses some of the highest-grade units of the orogenic belt. It is subdivided into three domains, the upper-amphibolite-facies Hartmann Domain in the north, the lower amphibolite-facies Khumib Domain in the center, and the upper amphibolite- to granulite-facies Hoarusib Domain in the south (Goscombe et al., 2003b, 2005a; Seth et al., 2008; Jung et al., 2014). The dominant unit is composed by metasedimentary rocks from the Damara Supergroup, but Proterozoic basement slivers are interspersed within the Orogen Core, especially in its southern portion, and both were intruded by abundant acidic magmas along its entire length during the Neoproterozoic (Seth et al., 1998; Kröner et al., 2004; Konopásek et al., 2008; Janoušek et al., 2010). The western portion of the Orogen Core was profoundly affected by the Three Palms Shear Zone, a wide network of transpressive sinistral shear zones that include several branches, such as the Hartmann, Village and Khumib mylonitic zones. Rocks associated with the Coastal Terrane (see below), including remnants of Tonian orthogneisses, predominate to the west of the Three Palms Shear Zone, but may also occur in between some of its individual branches (Konopásek et al., 2008, 2014; Oriolo et al., 2018).

Finally, the westernmost domain of the Kaoko Belt is the Coastal Terrane. It stretches from the Three Palms Shear Zone to the Atlantic Ocean and consists of a long-lived magmatic system associated with a varied association of ortho- and paragneisses. The metasedimentary units of the Coastal Terrane are relatively more juvenile and show less of a Congo cratonic provenance signature than the rest of the Kaoko Belt (Konopásek et al., 2014; Goscombe et al., 2018). The terrane also

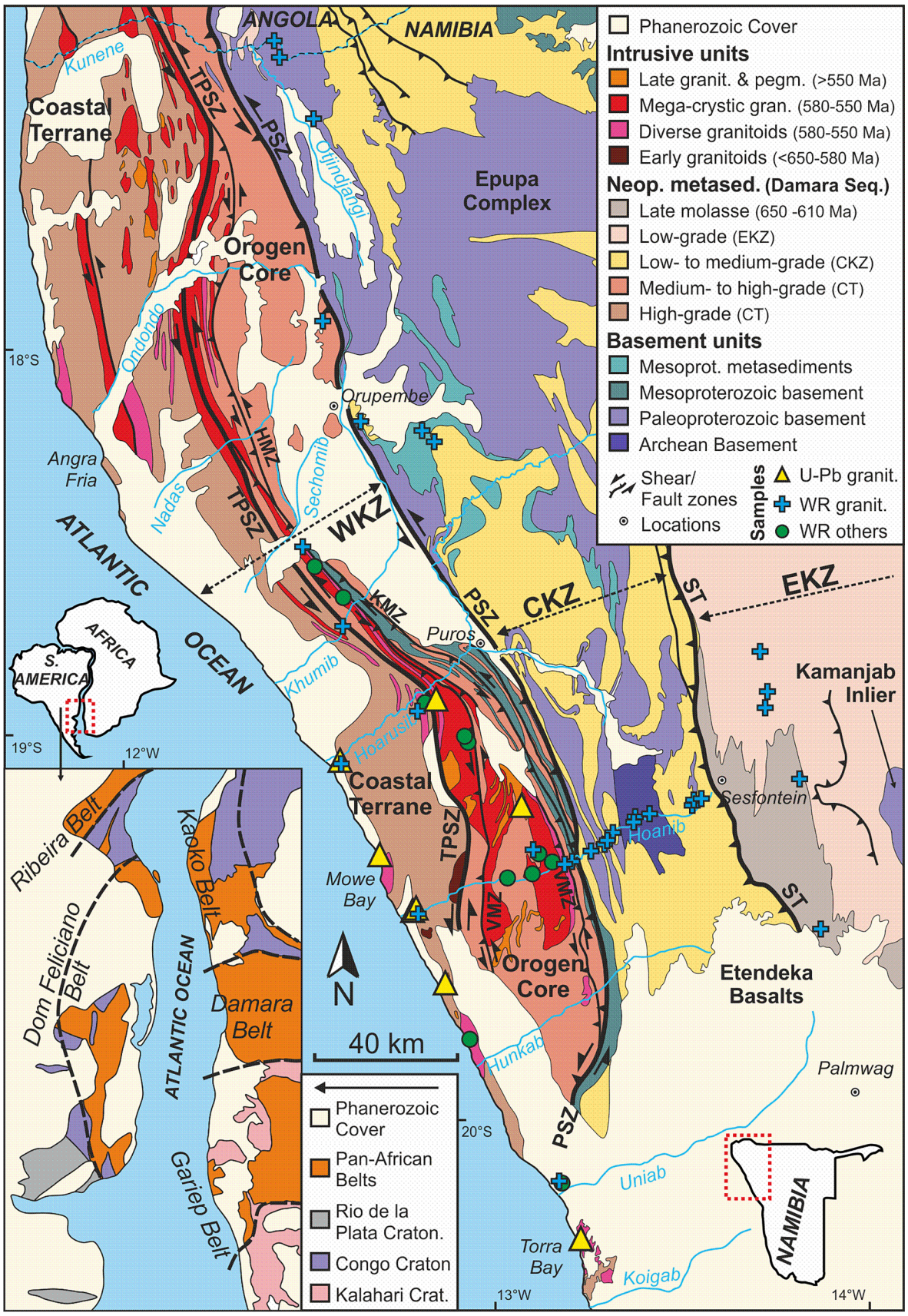

Fig. 1. Geological map of the Kaoko Belt with location of analyzed samples, and connection between South American and African Pan-African orogenic belts in a post-Gondwana break-up situation (inset). WKZ/CKZ/EKZ – Western/Central/Eastern Kaoko Zone; TPSZ/PSZ: Three Palms/Puros Shear Zone; HMZ/KMZ/VMZ: Hartmann/Khumib/Village Mylonitic Zone; ST: Sesfontein Thrust; CT: Coastal Terrane; OC: Orogen Core; WR: Whole-rock. Modified from Goscombe & Gray (2008), Jung et al. (2009), and Kröner et al. (2015).

includes the main occurrences of Tonian orthogneisses and early-Pan-African granitic rocks as old as 650 Ma in the Kaoko Belt (*e.g.,* Konopásek et al., 2020), both of which correlate with the easternmost units of the Dom Feliciano Belt in South America (Seth et al., 2000, 2008; Frimmel et al., 2011; Oyhantçabal et al., 2011; Konopásek et al., 2016, 2018; Basei et al., 2018; Will et al., 2020; Silva Lara et al., 2022).

In addition to these four domains, the Pan-African rocks immediately to the south of the Etendeka Plateau, known as Ugab Zone, are also sometimes considered part of the Kaoko Belt in its interference zone with the northern Damara Belt (*e.g.,* Goscombe et al., 2018). This area is not considered in this contribution for two reasons: first, the tectonic subdivision of the Kaoko Belt does not apply to the Ugab Zone, thus restricting the aims of this contribution; second, the magmatism intrusive in the Ugab zone is much more strongly associated, from a geochronological perspective, with that of the Damara Belt, which is younger than that of the Kaoko Belt (*e.g.,* Seth et al., 2000; Masberg et al., 2005; Passchier et al., 2007; Jung et al., 2009; Schmitt et al., 2012).

The tectonic evolution of the Kaoko Belt was a multi-stage process. The Coastal Terrane has an older orogenic history than the rest of the system, recording high-grade metamorphism and magmatism from *ca.* 650 Ma until 590 Ma. It has been often interpreted as a magmatic arc during this period (*e.g.,* Goscombe & Gray, 2007; Konopásek et al., 2014), though this has been challenged more recently in favor of an intracontinental evolution (Konopásek et al., 2020; Janoušek et al., 2023, more details in section 5.3). At *ca.* 590 to 580 Ma, the Coastal Terrane was thrust southeastwards onto the rest of the Kaoko Belt, accompanied by widespread transpression and regional metamorphism between 580 and 550 Ma. This was followed by late-stage shear-zone reactivation and magmatism associated with the extrusion of the orogenic core, juxtaposing terranes that record starkly contrasting metamorphic conditions (Goscombe et al., 2005a, 2017). In this context, the main shear zones between the individual terranes of the belt are interpreted alternatively as early terrane boundaries from 580 Ma onwards (Goscombe & Gray, 2008; Foster et al., 2009) or as the result of strain localization during the late stages of the orogeny after *ca.* 550 Ma (Konopásek et al., 2005; Ulrich et al., 2011).

2.2. *Pan-African magmatism*

Granitic intrusions are a significant part of the geological history of the Kaoko Belt. They do not occur in the Eastern and Central Kaoko zones, but are restricted to the two terranes that comprise the Western Kaoko Zone, namely the Orogen Core and Coastal Terrane. There,

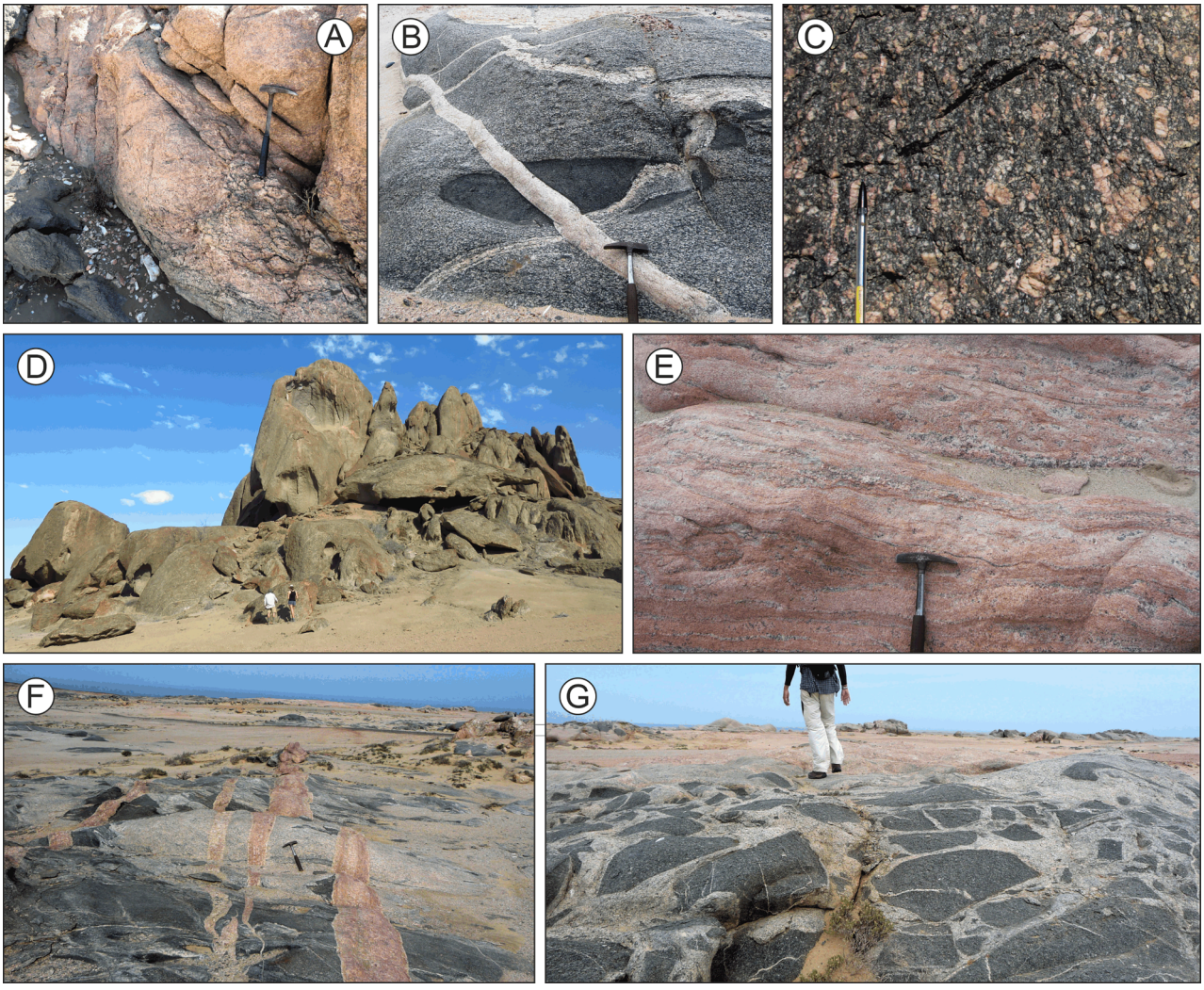

Fig. 2. Field aspects of Pan-African granitoids of the Kaoko Belt. A: Leucocratic granitoid intrusive into muscovite-quartz schist in the Orogen Core (OC); B: mafic magmatic enclave hosted in biotite-rich granodiorite, cut by late leucogranitic dyke, Tora Bay, Coastal Terrane (CT); C: Undeformed megacrystic granite with K-feldspar phenocrysts, OC; D: granitic inselberg, OC; E: magmatic banding in pink leucocratic granite grading into pegmatite, CT; F: Late pink granitoid dykes with magmatic banding, CT; G: swarm of mafic magmatic enclaves in hornblende- and biotite-bearing grandiorite, CT. (For interpretation of the references to color in this figure legend, the reader is referred to the web version of this article.)

however, they constitute as much as *ca.* 20 % of the area of the orogen (Goscombe et al., 2018). Apart from larger, mappable plutons and stocks, they also occur as countless bodies too small for the scale of geological maps within metasedimentary and basement associations (Fig. 2A). Larger intrusive bodies are particularly common close to the various sprays of the Three Palms Shear Zone, along which they are elongated following the NNW-SSE lineament of the Kaoko Belt, in some cases over tens or even hundreds of kilometers.

The earliest Pan-African granites within the Kaoko Belt occur in the Coastal Terrane. An age of 656 ± 8 Ma (U-Pb zircon evaporation) reported by Seth et al. (1998) for a monzogranitic augengneiss along the Hoanib section might represent an early magmatic pulse, though similar ages have been interpreted as high-grade metamorphism of Tonian to Cryogenian basement in equivalent units in the Dom Feliciano Belt in South America (Oyhantçabal et al., 2009; Basei et al., 2011a; Lenz et al., 2011; Will et al., 2019; Silva Lara et al., 2022). The best-studied magmatic association in the Coastal Terrane is the Angra Fria Magmatic Complex (Konopásek et al., 2016; Janoušek et al., 2023), which comprises two suites with different ages but relatively similar compositions ranging from gabbroic to granitic. The older suite has ages between 626 and 620 Ma and is variously deformed, whereas the younger suite was emplaced between 586 and 574 Ma and preserves a weak magmatic foliation, with only localized sub-solidus overprint. Other well-studied granitic associations from the Coastal Terrane are the Nk Pluton and the Torrabaai–Koigabmond Complex in the Tora Bay region (Fig. 2B, Masberg et al., 2005; Jung et al., 2009). The former comprises fine- to medium-grained granodioritic to granitic gneiss associated with numerous granitic veins, whereas the latter includes an association of different intrusions comprising undeformed quartz-diorite, granodiorite and leucogranite. The best age constraint for the Torrabaai–Koigabmond Complex is *ca.* 550 Ma, based on U-Pb analyses of both zircon and monazite (Jung et al., 2009), which also provides a younger estimate for the crystallization age of the deformed Nk pluton. Other granites and orthogneisses from the Coastal Terrane yielded U-Pb zircon ages between *ca.* 575 and 560 Ma (Seth et al., 1998; Franz et al., 1999).

Moving towards the eastern portion of the Western Kaoko Zone, the abundant granodiorite to granite bodies emplaced along the various sprays of the Three Palms Shear Zone are grouped into the Boundary Igneous Complex (Konopásek et al., 2008; Janoušek et al., 2010). Within this complex, the megacrystic melanocratic granite and granodiorite of the Amspoort Intrusive Suite are the most characteristic intrusive rocks of the Kaoko Belt, being distinguished by their porphyritic texture with centimetric K-feldspar phenocrysts and varied degrees of solid-state deformation (Fig. 2C, D). Other varieties included in the complex are fine- to medium-grained felsic granitoids (Janoušek et al., 2010). Magmatic ages range from *ca.* 580 to 550 Ma, the youngest of which are from granite bodies that were affected by late local shear zones (Seth et al., 1998; Kröner et al., 2004; Goscombe et al., 2005b; Konopásek et al., 2008). The tectonic position of the Boundary Igneous Complex within the Kaoko Belt is somewhat ambiguous, as it is strongly linked to the wider domain of the many interlinked sprays of the Three Palms Shear Zone, the easternmost of which is the Village Mylonitic Zone (Konopásek et al., 2008; Oriolo et al., 2018). This section of the Western Kaoko Belt includes rocks that are associated with both the Orogen Core and the Coastal Terrane (Konopásek et al., 2008, 2014; Goscombe et al., 2018). Both the Coastal Terrane and the Orogen core are cross-cut by numerous post-tectonic pegmatitic veins (Fig. 2 E, F), in which Goscombe et al., (2005b,2018) recognize three generations with different orientations at *ca.* 530, 515 and 508 Ma.

3. Samples and methods

In order to investigate the variety of geochemical and isotopic signatures in the Pan-African granitoids of the Kaoko Belt and investigate the possible sources involved in their genesis, we compiled a large dataset including new analyses performed in samples collected throughout the belt, as well as data published over the past three decades. The novel dataset includes results from a total of 33 samples of granitoids and subordinate associated basic rocks from the Western Kaoko Zone, representing units from both the Coastal Terrane and Orogen Core. Almost all samples were analyzed for major and trace elements and Sr-Nd isotopes, and 12 samples were also dated by U-Pb in zircon using the LA-ICP-MS method, in order to detail the intrusive history of these units. Details on the location and characterization of each sample are given in the Supplementary Material A, as well as a listing of the methods applied to each sample, whereas details on the analytical methods applied in this study are presented in the Supplementary Material B. The geochemical and isotope dataset of the granitoids was complemented with data from the literature, including subordinate associated basic rocks, mostly from detail petrogenetic studies (Masberg et al., 2005; Konopásek et al., 2008, 2016; Jung et al., 2009; Janoušek et al., 2010, 2023), as well as a few more samples from regional studies (Seth et al., 1998, 2002; Kröner et al., 2004; Jung et al., 2014).

As discussed above, the limits between both the Coastal terrane and the Orogen Core are ambiguous, due to the pervasive effect of the Three Palms Shear Zone. In the organization of our dataset, we consider all granites between the Puros Shear Zone and the westernmost spray of the Three Palms Shear Zone (Fig. 1) to correspond to the Orogen Core, including the granites commonly associated with the Boundary Igneous Complex (Konopásek et al., 2008; Janoušek et al., 2010). Data on 13 new samples from the Orogen Core come predominantly from this complex, representing both its megacrystic (Amspoort-type) and equigranular leucocratic units, and were collected between the Sechomib and Hoanib sections of the belt. The remaining 20 new samples represent granites from the Coastal Terrane, and correspond to a diverse set of magmatic units ranging from tonalite to leucogranite. While some samples come from the eastern portion of the Coastal Terrane along the Hoarusib River, most samples are from the Skeleton Coast, covering an expanse approximately between Möwe Bay and Torra Bay. Because the Coastal terrane counts with a high number of analyses (20 new samples, added to a dataset of *ca.* 100 samples compiled from the literature) and spreads over a large geographic area, we subdivide this dataset into three geographic regions. This subdivision is useful to identify eventual regional variations in the sources involved in the generation of the units (see section 5). The northern portion encompasses the Angra Fria Magmatic Complex studied by Janoušek et al. (2023) in the homonymous locality (Fig. 1). The central portion corresponds broadly to the region between the Hoarusib and Hunkab rivers, and is almost entirely represented by the new dataset. Finally, the southern portion of the Coastal Terrane represented in this dataset extends approximately from the Uniab to the Koigab rivers, and includes the units around Torra Bay studied by Masberg et al. (2005) and Jung et al. (2009), besides new samples analyzed in this study.

In addition to the data collected from the Pan-African magmatic granitoids, 49 samples of basement rocks and metasedimentary rocks from the Damara Supergroup were also analyzed for isotope geochemistry. They provide a more detailed characterization of the isotopic signature of regional units within the belt, which can then be compared to the intrusive units. Of these, 17 samples correspond to basement units: six from the Eastern Kaoko Zone, mostly gneiss and granite from the Kamanjab Inlier; and 11 from the Central Kaoko Zone, representing gneisses from the Epupa Complex and Archean to Paleoproterozoic inliers in the Hoarusib and Hoanib river sections. The remaining 32 samples represent metasedimentary rocks from all four domains of the Kaoko Belt, representing very low- to high-grade metamorphic units. As with the sampled granitoids, the location and the characterization of these samples are summarized in the Supplementary Material A. The regional isotope dataset was further complemented by data from the literature, compiled from Seth et al., (2002,2008), Goscombe et al., (2003b 2005b), Masberg et al. (2005), Goscombe & Gray (2007), Jung

et al., (2007,2012), Janoušek et al. (2010), Kröner et al. (2010), Konopásek et al., (2014,2017), and Kleinhanns et al. (2015). In order to allow for a meaningful comparison between the different units, and considering that not all analyzed granitoids have good age constraints, the isotope ratios $^{87}Sr/^{86}Sr_{(i)}$ and ε_{Nd} were (re-)calculated for the entire dataset for an age of 550 Ma, corresponding to the end of the main regional metamorphic event of the Kaoko Belt (section 2).

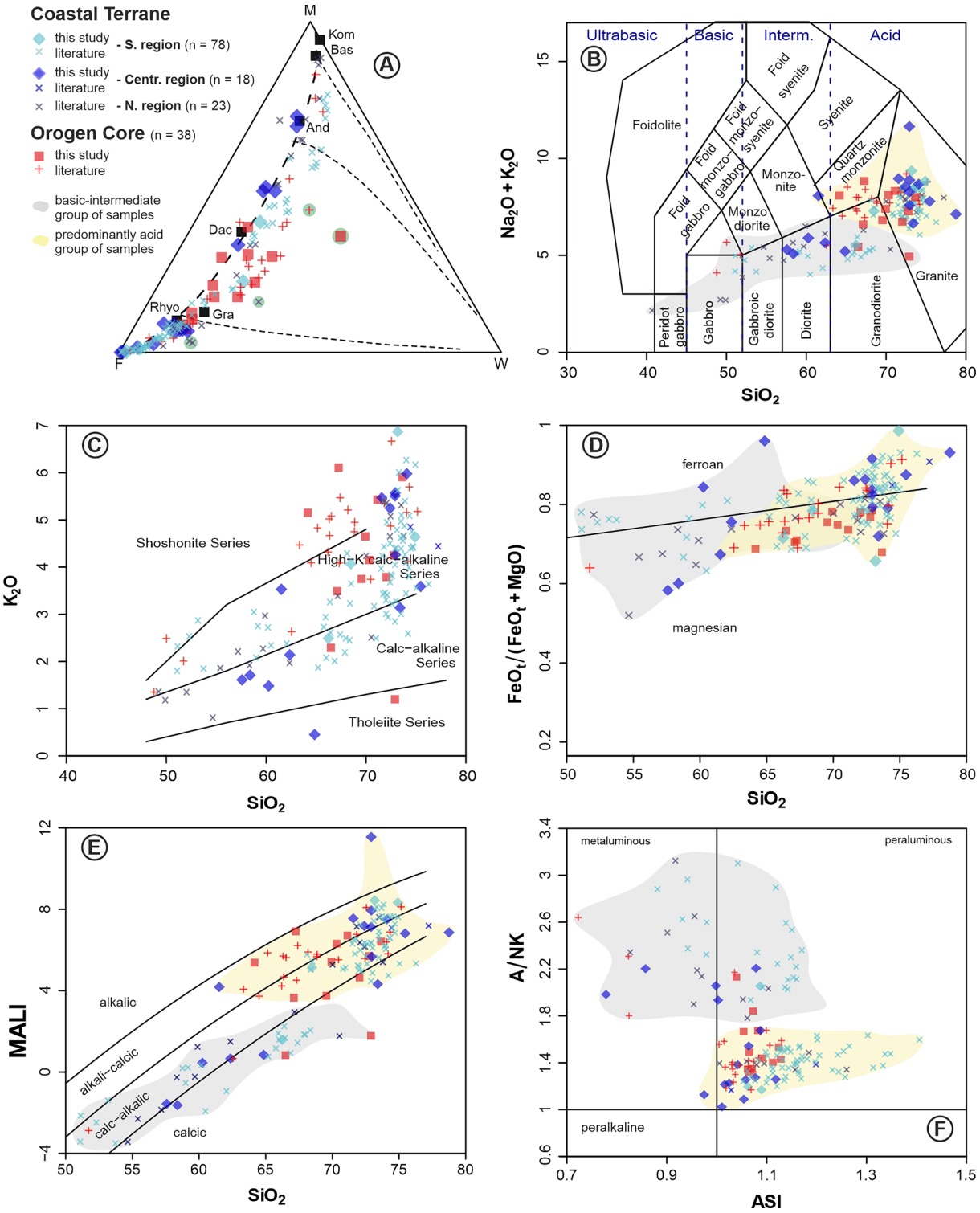

Fig. 3. Major-element classification of the Pan-African granitoids of the Kaoko Belt. A: Empirical F–M–W index of chemical weathering (fresh felsic igneous rocks, fresh mafic igneous rocks, and chemical weathering) of Ohta and Arai (2007). Samples falling furthest away from the un-weathered trendline are indicated with a green shade, and were discarded for the remaining plots in this figure; B: Modified wt. % SiO_2 vs. $Na_2O + K_2O$ classification diagram of Middlemost (1994); C: SiO_2-K_2O classification plot of Peccerillo & Talor (1976); D: SiO_2 vs. FeOt/(FeOt + MgO) plot of Frost et al. (2001); E: SiO_2 vs. Modified Alkali-Lime Index (MALI) diagram of Frost et al. (2001); F: ASI vs. A/NK binary plot of Shand (1943). See text for the origin of data compiled from the literature. Diagrams plotted using GCDKit (Janoušek et al., 2006). (For interpretation of the references to color in this figure legend, the reader is referred to the web version of this article.)

4. Results

4.1. Elemental geochemistry

Results from the new analyses are presented in the Supplementary Material C. Before the whole-rock geochemical data can be interpreted further, it is important to consider the potential impact of the low-grade metamorphic overprint and solid-state deformation that affected many magmatic units of the Kaoko Belt. In addition to having taken samples predominantly from little-deformed zones of the investigated outcrops, we followed the approach of Janoušek et al. (2023) in testing eventual modifications of the original major-element contents using the ternary

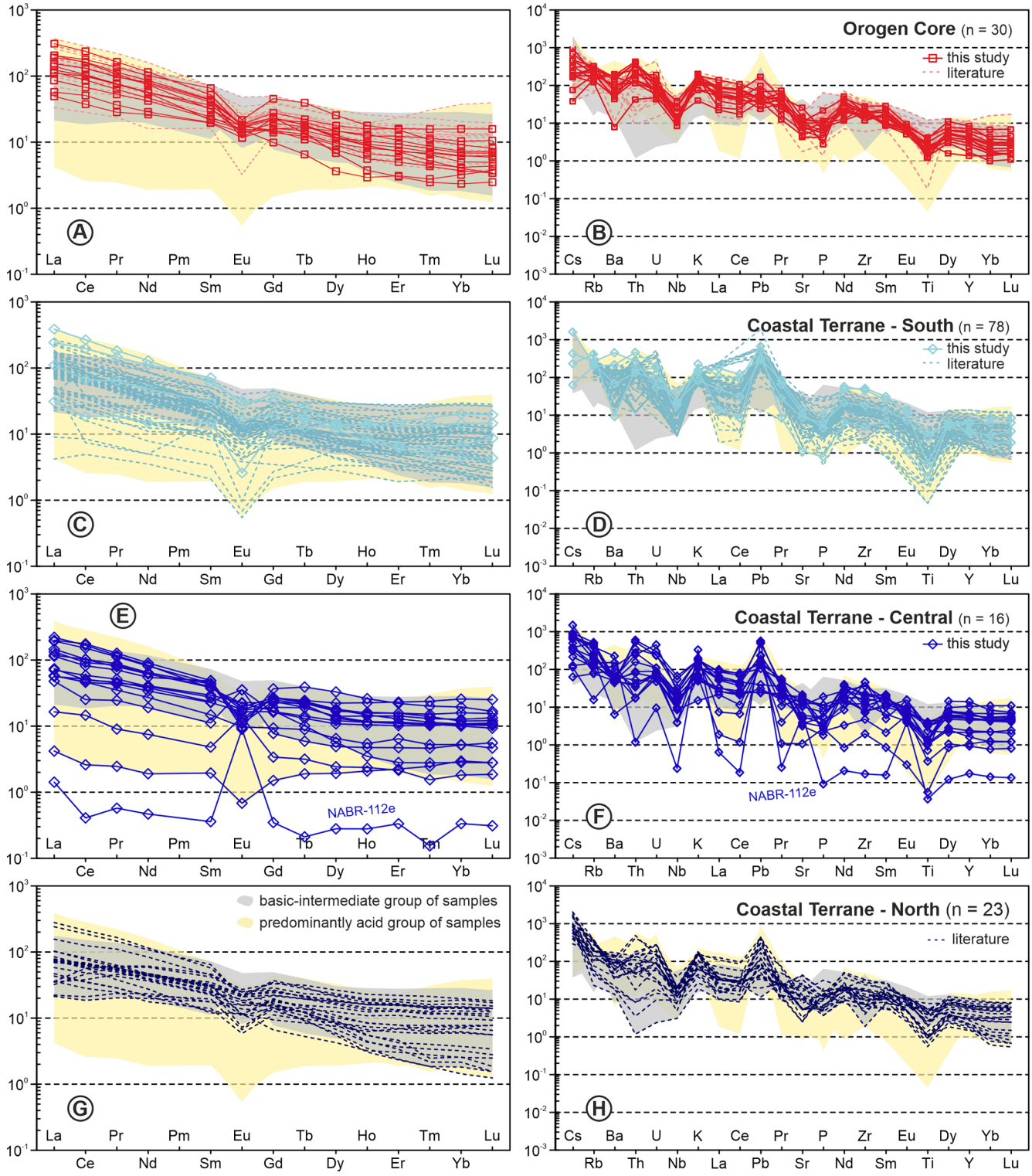

Fig. 4. Normalized multi-element diagrams of different subsets of the Pan-African granitoids of the Kaoko Belt. A, C, E, G: Chondrite-normalized (Boynton, 1984) REE patterns; B, D, F, H: Primitive mantle-normalized (Sun & McDonough, 1989) trace elements. All plots are compared to the total variation of predominantly basic-intermediate and acid composition groups, as defined in Fig. 3, except for individual outliers. See text for the origin of data compiled from the literature. Diagrams plotted using GCDKit (Janoušek et al., 2006).

plot for identification of chemical weathering of felsic and mafic igneous rocks of Ohta and Arai (2007). As most samples plot relatively close to the trend of un-weathered igneous rock (Fig. 3A), we assume that using the whole-rock geochemical data for the interpretation of the magmatic evolution of the analysed rocks is reasonable, even if minor alteration cannot be completely ruled out in some instances. In this sense, the five samples that fall furthest away from the un-weathered trendline (Fig. 3A) were discarded from subsequent consideration in terms of their more mobile major-element compositions. Overall, the compiled dataset includes rocks with SiO_2 contents that mostly range from *ca.* 40 to 78 %, with basic to intermediate compositions coming from a subordinate group of samples of gabbroid and tonalitic enclaves associated with the granitoids (*e.g.,* as reported by Janoušek et al., 2010, 2023, illustrated in Fig. 2B, G). These samples form a group that, with the inclusion of a few more differentiated compositions, consistently yields geochemical signatures that are different from the rest of the compilation (see Fig. 3B-H). Overall, in the total alkalis vs. silica (TAS) plot (Middlemost, 1994), a majority of samples plot within the granite, granodiorite, and quartz monzonite fields, with only a subordinate number of diorite and gabbro compositions (Fig. 3B). There is a predominance of calc-alkaline to high-K calc-alkaline compositions in the SiO_2 vs. K_2O plot of Peccerillo & Taylor (1976), with lowest K_2O values constrained to the basic-intermediate group of samples (Fig. 3C). The slight tendency of more acid samples to advance into the shoshonitic field and towards more ferroan compositions in the SiO_2 vs. $FeO_t/(FeO_t + MgO)$ plot of Frost et al., (2001, Fig. 3D),observed in near-minimum melt compositions, is a typical feature of highly differentiated granitoids. Otherwise, there is a clear predominance of compositions plotting in the magnesian field. On the other hand, calc-alkalic to alkali-calcic signatures predominate for the entire dataset in the SiO_2 vs. Modified Alkali-Lime Index (MALI) diagram of Frost et al. (2001), with a subordinate group of calcic to calc-alkalic samples corresponding to the group of basic-intermediate samples (Fig. 3E). Finally, in the ASI vs. A/NK binary plot of Shand (1943), there is a predominance of slightly to moderately peraluminous signatures, followed by a separate cluster of metaluminous to weakly peraluminous compositions associated with more basic samples (Fig. 3F).

Overall, there are not many notable distinctions between the signatures of the granitoids from the Orogen Core and the Coastal Terrane, or between the different regions of the Coastal Terrane, in the diagrams described above (Fig. 3). The southern portion of the Coastal Terrane, for instance, is somewhat more ferroan and peraluminous than the rest of the dataset, in addition to a slight high-K calc-alkaline affinity, though there is still a meaningful overlap with results from other domains of the belt.

Chondrite-normalized REE plots (Boynton, 1984) are shown in Fig. 4, distinguishing between samples from the Orogen Core and the different regions of the Coastal Terrane, and between new and published data. The total range of the entire dataset is also represented in each diagram, excluding strong outliers (see below), and differentiating between the two groups of samples established in Fig. 3, *i.e.,* predominantly basic-intermediary and predominantly acid. Considering the size of the dataset, the variations in the observed signatures between the different groups are not especially large. In particular, the samples from the Orogen Core and from the northern sector of the Coastal Terrane have similar signatures with normalized contents varying within an order of magnitude, always above unity. Both have signatures that predominantly have a moderate fractionation, though two samples of possible amphibole cumulates from the northern Coastal Terrane analyzed by Janoušek et al. (2023) stand out for their convex-upwards patterns. The southern and central portions of the Coastal Terrane, on the other hand, have more heterogeneous signatures, with normalized contents varying within a range of almost two orders of magnitude, and including some samples with overall depleted values that do not straddle above a few tens of units. The predominant fractionation trend is still moderate, though a group of samples from the central portion of the Coastal Terrane yield almost flat patterns (seven samples with $La_N/Yb_N < 6.00$). In general, lower La_N/Yb_N ratios are mostly associated with the group of basic-intermediate samples, though the contrast is not as clear as with major-element signatures (Fig. 3). The Coastal Terrane also includes the clearest outlier of the entire dataset, sample NABR-112e, which is a pegmatitic granitoid characterized by strongly depleted REE values (mostly below unit) and an extreme positive Eu anomaly ($Eu/Eu^* = 24.4$). For the rest of the dataset, Eu anomalies are mostly negative, ranging from moderate to strong, particularly in the Orogen Core (median Eu/Eu^* of 0.59) and in the southern portion of the Coastal Terrane (median Eu/Eu^* of 0.58). By comparison, the anomalies of the northern Coastal Terrane (Angra Fria Magmatic Complex) are more moderate (median Eu/Eu^* of 0.72), whereas a subordinate population of samples from the central portion of the same terrane have positive anomalies (four samples with $Eu/Eu^* > 1$).

Primitive mantle-normalized trace element diagrams (Sun & McDonough, 1989) are also shown in Fig. 4, following the same organization as the one for REE data. For this diagram, individual analyses from Masberg et al. (2005) and Jung et al. (2009) that did not include some crucial elements (*e.g.,* U, Th) were discarded. In general, the most notable patterns are enrichments in LILE (Cs, Rb, Ba, K), as well as U and Th, and depletions in some HFSE (Nb, Ti) and P. Note that Ta was not plotted in this diagram, in order to keep an internal consistency of the dataset, as it was not analyzed in the samples from the southern Coastal Terrane compiled from published data. However, negative anomalies of the element are also very common in the available dataset, as observed before in the Amspoort Intrusive Suite and Angra Fria Magmatic Complex (Janoušek et al., 2010, 2023). There are slight differences in a comparison between the different terranes, as samples from the Orogen Core typically have the flattest patterns of the dataset, whereas the anomalies (both positive and negative) are more pronounced in the Coastal Terrane (particularly in its southern and central sectors), which is also reflected in the relative range of compositions observed for the different terranes. The same sample that produced an outlying pattern in the REE diagram (sample NABR-112e) also deviates from the typical trace elements signatures, displaying more pronounced negative anomalies and more depleted compositions in general.

4.2. Isotopic geochemistry

All results from the new analyses are presented in the Supplementary Material D. Fig. 5 presents a comparison of new and recalculated $^{87}Sr/^{86}Sr_{(550)}$ and $\varepsilon_{Nd(550)}$ values, in order to illustrate the signatures of the main regional units of the Kaoko Belt at the time of the regional magmatism and interrogate their influence as possible crustal sources. Because the different basement units have varying pre-Pan-African geological evolutions, it should be noted that the long-term stability of the isotopic signatures of these units prior to 550 Ma is less robust for the more mobile Rb-Sr system than for the Sm-Nd system. $^{87}Sr/^{86}Sr_{(550)}$ ratios from granitoids range widely from *ca.* 0.695 to 0.720, whereas $\varepsilon_{Nd(550)}$ values are predominantly between −10 and −2 (Fig. 5). Both parameters indicate a participation of ancient crustal material during the genesis of the granites, while excessively low $^{87}Sr/^{86}Sr_{(550)}$ ratios (*i.e.*, below 0.6989) are likely caused by over-recalculation from recent Rb and/or Sr disturbances. There are only three samples with positive $\varepsilon_{Nd(550)}$ values, two rocks with tonalitic and granitic compositions from a single outcrop of the central region of the Coastal Terrane characterized by abundant mafic enclaves, and one from a mafic dolerite from the Orogen Core analyzed by Janoušek et al. (2010). Most of the samples from the southern region of the Coastal Terrane correspond to those from the Nk Pluton and Torrabaai–Koigabmond Complex analyzed by Masberg et al. (2005) and Jung et al. (2009). They cover a compositional range that stands apart from the remaining groups by having the lowest $\varepsilon_{Nd(550)}$ values and relatively low $^{87}Sr/^{86}Sr_{(550)}$ ratios. In comparison, the other groups (Orogen Core and central and northern portions of the Coastal Terrane) have predominantly overlapping signatures.

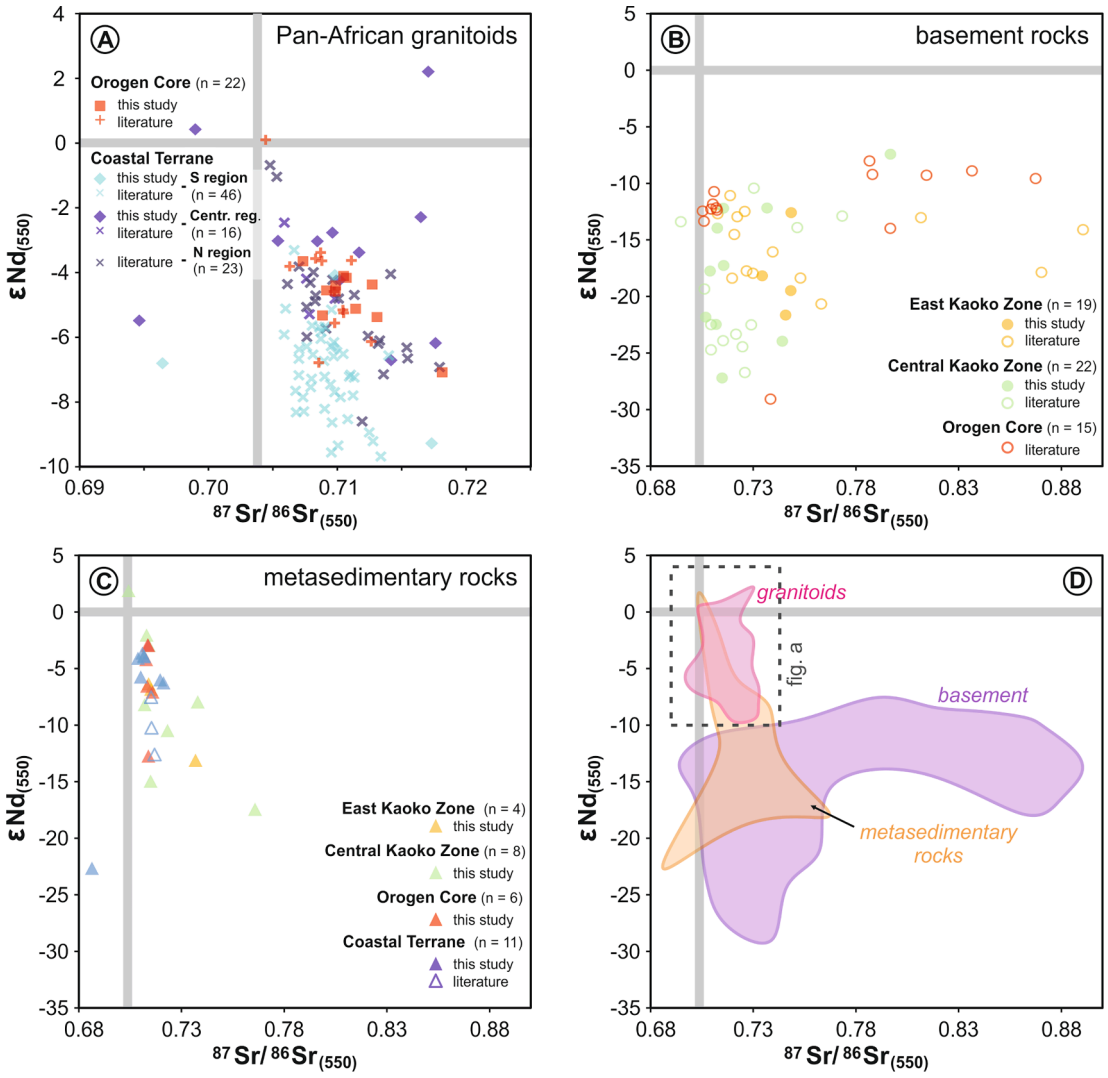

Fig. 5. Sm-Nd signatures of the Pan-African granitoids of the Kaoko Belt and regional associations, separated by tectonic domain. A: data from granitoids; B: data from basement associations; C: data from metasedimentary rocks; D: comparison of the compositional field of the main regional lithological types shown in a, b, and c. See text for the origin of data compiled from the literature.

On the other hand, the remaining lithological groups of the Kaoko Belt have much broader compositional ranges (Fig. 5). Basement rocks have $^{87}Sr/^{86}Sr_{(550)}$ values that mostly range from 0.705 to 0.880, whereas $\varepsilon_{Nd(550)}$ ratios are between −7 and −29. There are general differences between the signatures of different basement associations. The basement of the Eastern Kaoko Zone, which mostly corresponds to samples from the Kamanjab Inlier, is characterized by more elevated $^{87}Sr/^{86}Sr_{(550)}$ ratios and more radiogenic $\varepsilon_{Nd(550)}$ signatures (predominantly from 0.712 to above 0.800, and from –22 to −11, respectively). These ranges partially overlap with the signatures of basement samples from the Orogen Core, which are mostly represented in the compilation by Mesoproterozoic orthogneisses and their host rocks (Jung et al., 2012). That said, the there is a predominance of more radiogenic $\varepsilon_{Nd(550)}$ ratios (mostly between −8 and −15) in the latter. On the other hand, basement samples from the Central Kaoko Zone, comprising both Archean and Paleoproterozoic basement slivers, the latter coming from the Epupa Complex, yield $^{87}Sr/^{86}Sr_{(550)}$ ratios mostly between 0.706 and 0.766 and $\varepsilon_{Nd(550)}$ values from −28 to −7. The compositional range of the metasedimentary rocks from all domains of the Kaoko Belt occupies a somewhat intermediate position between the signatures of the basement rocks and granitoids, with about half of the results overlapping with the field delimited for the Pan-African magmatism and the rest spreading out to other areas of the plot.

The main first-order differences observed between the major units of the Kaoko Belt are also evident in Nd evolution diagrams (Fig. 6) following de Paolo (1981). Both single-stage and two-stage Nd T_{DM} model ages following Liew & Hofmann (1988) were calculated for the analyzed granitoids (Supplementary Material D), as the latter approach is commonly recommended for granitic rocks in order to correct for trace-mineral-controlled fractionation of $^{147}Sm/^{144}Nd$ during fractional crystallization and partial melting (*e.g.,* Janoušek et al., 2016; Bea et al., 2023). While the calculated model ages of most samples do not vary greatly between both calculating approaches, individual samples with elevated $^{147}Sm/^{144}Nd$ ratios lead to outlying old single-stage model ages. Hence, we prefer the use of two-stage model ages for the analyzed granitoids (Fig. 6), as it corrects for these outliers while still using a consistent approach to the calculation of the entire dataset, without incurring in significant changes for the rest of the dataset. This is in accordance with most recent recommendations (Janoušek et al., 2016; Bea et al., 2023). In this diagram it is evident that all units of the Kaoko Belt yield model ages indicative of long crustal residence times, with the overwhelming majority of samples yielding Paleoproterozoic and Archean model ages. Basement units have the oldest overall signatures, with the possible exception of the restricted basement within the Coastal Terrane, which includes Tonian associations for which there are little available data. Metasedimentary rocks yield particularly scattered data,

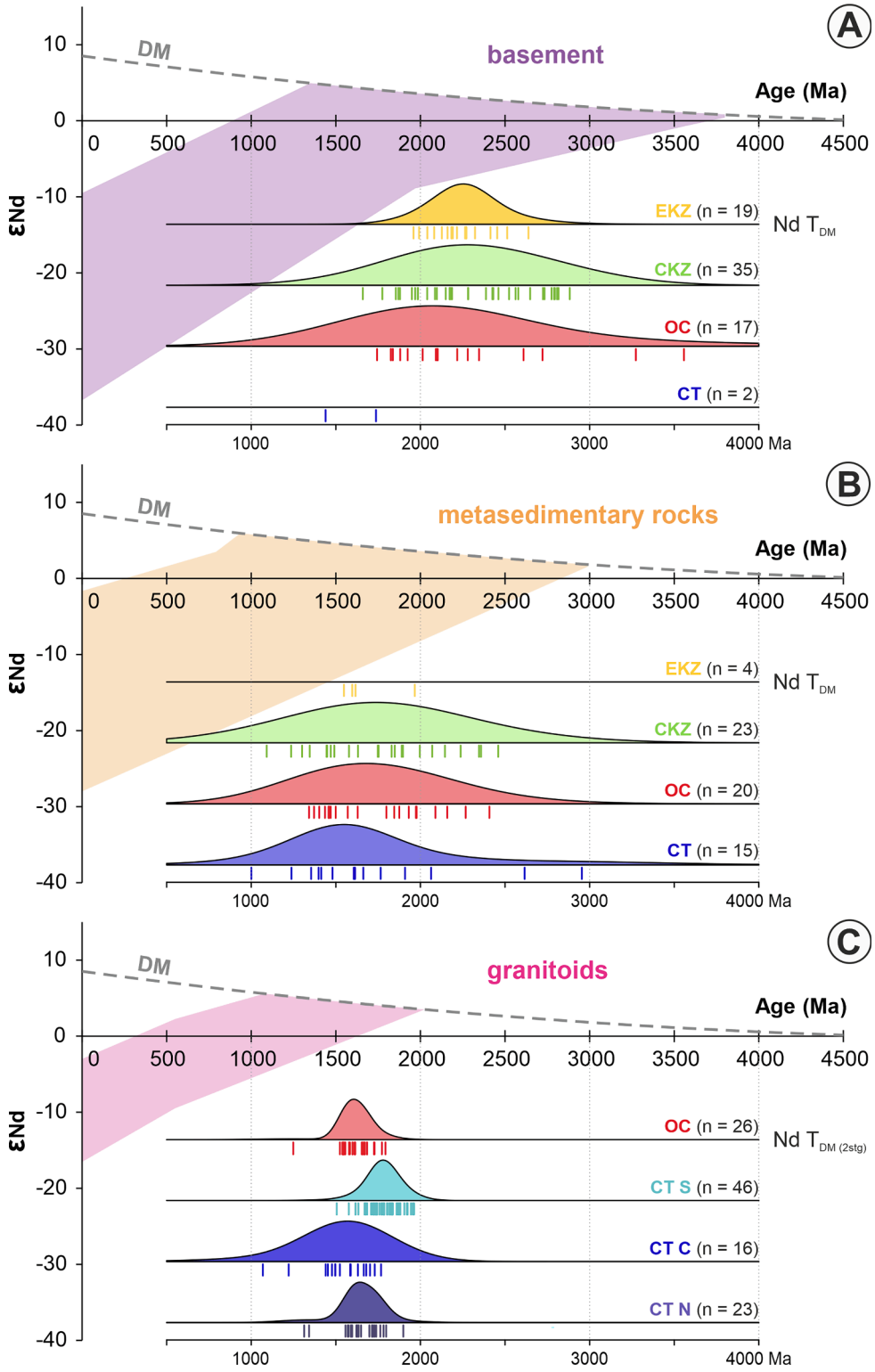

Fig. 6. Nd evolution diagrams (following de Paolo, 1981) for the Pan-African granitoids of the Kaoko Belt and regional associations. See text for the origin of data compiled from the literature. EKZ/CKZ – Eastern/Central Kaoko Zone, OC – Orogen Core, CT – Coastal Terrane.

but they result, in general, in Nd T_{DM} model ages that are younger than those for their immediate basement. On the other hand, the analyzed granitoids yielded the most sharply defined signatures, with Nd $T_{DM\ 2stg}$ model ages basically restricted to the Paleoproterozoic. By comparing the different granitoids with one another, there seems to be a slight tendency of older signatures for the southern portion of the Coastal Terrane, for which most model ages are Siderian (2.5 – 2.3 Ga).

4.3. Zircon U-Pb

A total of 12 samples of granitoids from the Kaoko Belt were selected for zircon U-Pb dating using the LA-ICP-MS method. Two samples are representative of the magmatism intrusive in the Orogen Core between the Hoanib and Hoarusib rivers, whereas the remaining ten samples correspond to granites from the Coastal Terrane sampled along the

Skeleton Coast. All spot analyses performed, and their corresponding interpretation, are presented in the Supplementary Material E. A summary of the results is presented in Fig. 7 and in the paragraphs below, whereas descriptions of the analyzed samples and zircon populations and detailed explanations of the interpretation of the analytical results of each sample are presented in the Supplementary Material F. Many of the analyzed samples resulted in individual single-crystal ages covering many tens of Myr, surpassing possible analytical causes for the distribution and requiring geological causes for overdispersion. Because of this, for most samples we present more than one possible solution for calculating pooled ages from our dataset, in order to represent different alternatives for the best central ages and associated uncertainties. For each sample, our preferred age is given in bold, with preference being given to concordia ages over mean ages, as they consider all radiogenic Pb/U and Pb/Pb ratios collectively (Ludwig, 2008). On the other hand, mean $^{206}Pb/^{238}U$ ages considering a more expansive selection of single-crystal analyses result in broader uncertainties that may be more representative of the actual uncertainties involved in dating these samples (Fig. 7).

The two samples from the Orogen Core come from the Boundary Igneous Complex, consisting of fine- to medium-grained (sample *NABR-31*, **557.6 ± 4.5 Ma**/529.6 ± 8.2 Ma) and megacrystic (Amspoort Suite, sample *NABR-34*, **571.6 ± 1.8 Ma**/568.2 ± 8.2 Ma) varieties (Fig. 7). The preferred ages obtained for these samples are within the range of previously published ages for the complex (Seth et al., 1998; Kröner et al., 2004; Konopásek et al., 2008), and represent the intense magmatism that accompanied the regional metamorphism associated with transpression in the Kaoko Belt between 580 and 550 Ma, following the eastwards-oriented thrusting of the Coastal Terrane at *ca.* 590–580 Ma (*e.g.,* Goscombe et al., 2005a, 2017).

The results of samples from the Coastal Terrane range from *ca.* 595 to 555 Ma (Fig. 7). Though there is a clear predominance of ages older than the ones typically observed in the Orogen Core (*i.e.,* >580 Ma), capturing its older geological evolution relative to the rest of the Kaoko Belt, no rocks corresponding to the earliest magmatic stages in this terrane (650–620 Ma, Seth et al., 1998; Goscombe et al., 2005b; Konopásek et al., 2016) were dated. The oldest dated sample (*NABR-112a*, **594.9 ± 3.5 Ma**/592.4 ± 5.3 Ma) corresponds to a mafic enclave, identified in the field as an early magmatic stage in the corresponding outcrop. It is followed by a group of seven samples with partially overlapping ages between *ca.* 587 and 577 Ma: sample *NABR-113a*, tonalite with biotite and garnet, **587.1 ± 1.1 Ma**/579.3 ± 3.9 Ma; sample *NABR-114a*, biotite-bearing porphyritic granite, **583.3 ± 1.4 Ma**/581.2 ± 3.8 Ma; sample *NABR-112c*, tonalite, **582.7 ± 2.5 Ma**/579.3 ± 3.9 Ma; sample *NABR-106b*, biotite-bearing tonalite to granodiorite, **579.5 ± 3.4 Ma**/579.3 ± 4.2 Ma; sample *NABR-111*, coarse-grained pink leucogranite, **579.3 ± 8.7 Ma**/586 ± 12 Ma; sample *NABR-116b*, biotite granite with multiple mica-schist enclaves, **577.9 ± 2.0 Ma**/573.9 ± 6.1 Ma; and sample *NABR-116c*, biotite-bearing tonalite with mafic enclaves, **576.7 ± 1.2 Ma**/568.9 ± 6.2 Ma. The two youngest samples correspond to late granite-pegmatite veins with limited zircon content, resulting in less well-defined ages (sample *NABR-112e*, **555 ± 3 Ma**; sample *NABR-116d*, *ca.* **557 Ma**). The ages above are not only well within the range of ages previously published for the Coastal Terrane, but are also in accordance with the relative magmatic stratigraphy determined in the field for the two outcrops for which multiple samples were dated (NABR-112 and NABR-116, three samples each). In some cases, there can be an overlap between the pooled ages from the older samples and individual crystals interpreted as inherited in the younger samples, suggesting a partial recycling of older magmatic stages that is typical for protracted igneous evolutions (*e.g.,* Matzel et al., 2006; Miller et al., 2007; Schaltegger et al., 2009; Barboni et al., 2013), and which is well characterized in the correlated Florianópolis Batholith (Basei et al., 2021). Conversely, younger zircon populations in the oldest samples of these sets coincide with the age of the late pegmatite veins, suggesting a late- to post-magmatic disturbance of the isotopic system associated with this late magmatic stage.

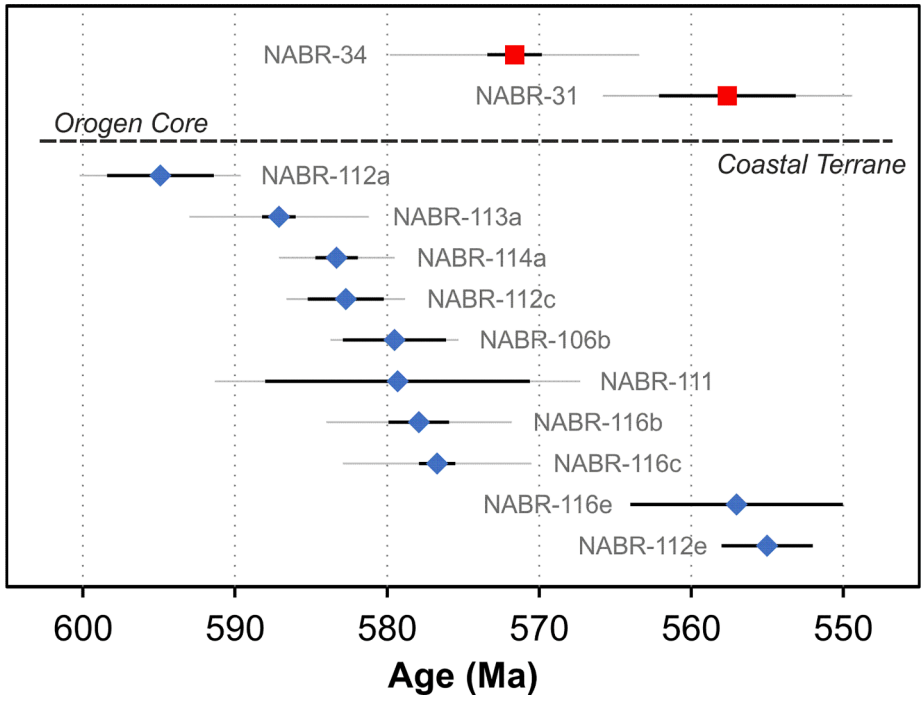

Fig. 7. Summary of new zircon U-Pb ages reported in this work. The ages plotted correspond to the preferred pooled age calculated for each sample (usually concordia ages) and their associated uncertainties. An additional (broader) error margin is also plotted, corresponding to the uncertainty calculated for weighted mean $^{206}Pb/^{238}U$ ages considering a more expansive selection of single-crystal analyses, which may be more representative of the actual uncertainties involved in dating these samples. Detailed descriptions of how each age was calculated and the entire U-Pb dataset are presented in Supplementary Materials F and E, respectively.

5. Discussion

5.1. South American connections of the Pan-African granitic magmatism of the Kaoko Belt

Understanding the petrogenesis of the Pan-African granitoids in the Kaoko Belt is critical for reconstructing the pre-Mesozoic configuration of tectonic units on either side of the South Atlantic Ocean, and thus for elucidating the formation of southwestern Gondwana. This is particularly true for the Coastal Terrane, which is probably the best candidate to link the basement geology of the southern portions of Africa and South America (*e.g.,* Frimmel et al., 2011; Oyhantçabal et al., 2011; Konopásek et al., 2016, 2018; Basei et al., 2018; Will et al., 2020; Silva Lara et al., 2022). This correlation encompasses similarities between the magmatism of the Coastal Terrane and the coeval Florianópolis Batholith in the Dom Feliciano Belt, as well as associated basement and (meta-) sedimentary units. A recent contribution by Janoušek et al. (2023) compares in detail, including in petrogenetic terms, a set of granitoids from the Coastal Terrane (Angra Fria Magmatic Complex) and a selection of rocks from the Florianópolis Batholith in the Dom Feliciano Belt (mostly in the Porto Belo Peninsula, South Brazil). The new data presented and compiled in this work, together with the wealth of data available from other units of the Florianópolis Batholith, allow us to expand this comparison in terms of geochronological and isotopic results (Fig. 8). The figure is based on the new dataset reported in this contribution, in addition to U-Pb data from Seth et al. (1998), Franz et al. (1999), Kröner et al. (2004), Goscombe et al., (2005b), and Konopásek et al., (2008,2016) for the Kaoko Belt, and Silva et al., (2002,2003,2005), Jelinek et al. (2005), Passarelli et al. (2010), Chemale et al. (2012), Florisbal et al., (2012a), Corrêa (2016), Basei et al. (2021), Peruchi et al. (2021), and Moraes et al. (2023) for the Florianópolis Batholith, and whole-rock isotopic geochemical data compiled from the same database used in Fig. 5 for the Kaoko Belt, in addition to data recalculated from Lopes (2008), Passarelli et al. (2011), Chemale et al. (2012), Florisbal et al., (2012b,c), Corrêa (2016), Hueck et al. (2016), Peruchi et al. (2021), and Moraes et al. (2023) for the Dom Feliciano Belt. The latter also includes units that comprise the regional context of the Florianópolis Batholith, which will be relevant for the discussion in the following sections.

A comparison of the U-Pb dataset for both domains (Fig. 8A) highlights some important similarities, in particular the prevalence of two main pulses of magmatic activity at *ca.* 620–610 and 590–580 Ma. They are recognized by the two main peaks in the KDE plots of single-crystal U-Pb ages, which are mirrored by the prevalence of pooled ages at the same time intervals. It is notable that apparent gaps in pooled ages shown in Fig. 8A, especially in the Kaoko Belt, are still represented in the KDE plots, suggesting that a subsumed magmatic activity persisted during this period, and is now preserved as inherited antecrysts that were likely recycled in later magmatic phases. This is a common feature of long-lived magmatic systems (*e.g.,* Matzel et al., 2006; Miller et al., 2007; Schaltegger et al., 2009; Barboni et al., 2013). This is especially notable for the conspicuous gap in pooled ages from the Kaoko Belt between *ca.* 610 and 595 Ma, an age interval that is only recorded by individual zircon crystals preserved in younger intrusive bodies. This period is not absent in the pooled ages from the Florianópolis Batholith as is the case in the Kaoko Belt, but it still represents a time of relatively less pronounced magmatic activity during the compared time period.

Another important distinction between both belts is that the early phase of magmatism (especially 640 – 600 Ma) is predominant in South America, whereas the later phases, between *ca.* 580 and 550 Ma, are much more prevalent in the Kaoko Belt. This latter period corresponds to the main regional metamorphic event in the belt following the thrusting of the Coastal Terrane at *ca.* 590–580 Ma (*e.g.,* Goscombe et al., 2005a, 2017), and was accompanied by widespread magmatism in both the Orogen Core and Coastal Terrane. In contrast, the equivalent period in the Dom Feliciano Belt is characterized by waning orogenic activity, with deformation progressively localizing into transcurrent shear zones, especially from 600 Ma onwards (Oriolo et al., 2016a; Hueck et al., 2018, 2020b). Intrusive magmatism, usually associated with late reactivations of the same shear zones, continued until *ca.* 570–560 Ma (*e.g.,* Oriolo et al., 2018; Lara et al., 2021; Silva Lara et al., 2022; Moraes et al., 2023) but subsequent magmatism, as young as 520 Ma, is mostly limited to individual intrusions and more abundant volcanism associated with late sedimentary basins (Sommer et al., 2005; Basei et al., 2011a, b; Matté et al., 2016). In contrast, post-570 Ma magmatism is much more common in the Kaoko Belt, as is best illustrated by the pooled ages

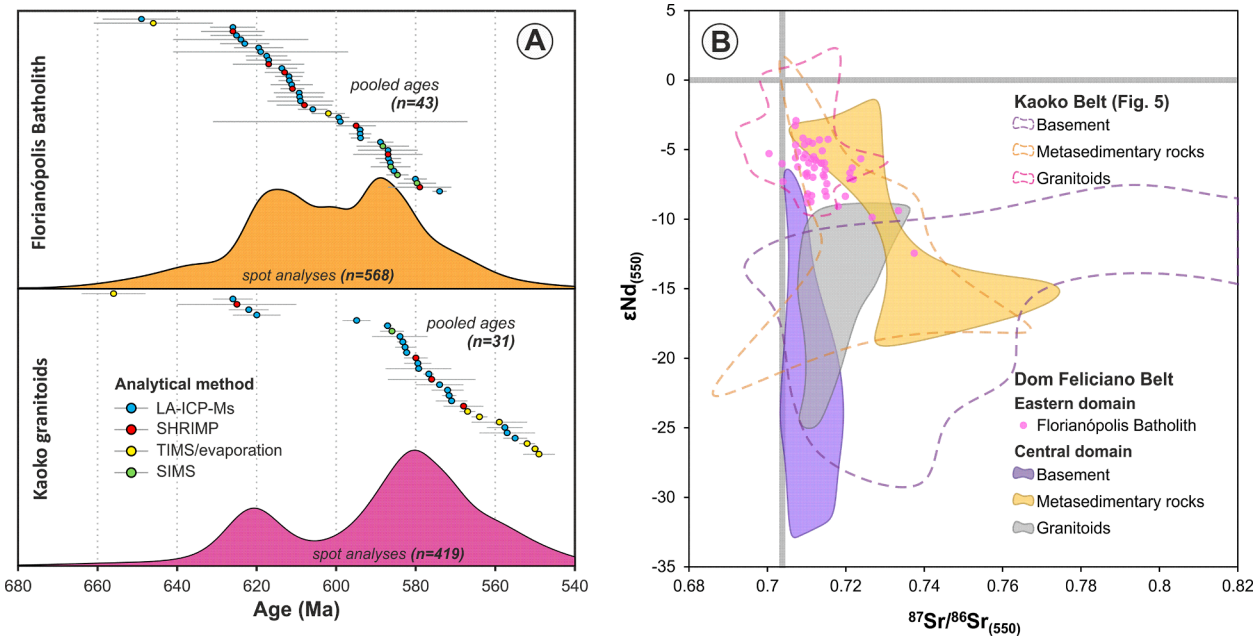

Fig. 8. Comparison of selected characteristics between the Pan-African granitoids of the Kaoko Belt and the Florianópolis Batholith of the Dom Feliciano Belt. A: pooled and single-spot U-Pb ages for the granitic magmatism emplaced between *ca.* 660 and 560 Ma, Kernel Density Estimates plotted using Density Plotter (Vermeesch, 2012). B: Sm-Nd signatures. See text for the origin of data compiled from the literature.

compiled in Fig. 8A. As most of these younger ages were acquired using zircon evaporation and thermal ionization techniques, this period is admittedly underrepresented in the compilation of single-spot U-Pb ages.

In addition to the U-Pb data, and expanding upon earlier comparisons (*e.g.,* Konopásek et al., 2016; Janoušek et al., 2023), the isotopic geochemistry of the Florianópolis Batholith also has distinctive similarities with the signatures obtained from the granitoids of the Western Kaoko Belt (Fig. 8B). Both granitic associations have overlapping ranges in terms of $\varepsilon_{Nd(550)}$ and $^{87}Sr/^{86}Sr_{(550)}$ values, although Nd signatures from the African granites are slightly more radiogenic (including a few positive $\varepsilon_{Nd(550)}$ values) then what is observed in South America. The similarities between both associations also expand to a comparison with other regional units of the Kaoko and Dom Feliciano belts. In particular, both the Florianópolis Batholith and the Neoproterozoic intrusive magmatism in the Kaoko Belt have notably more juvenile signatures than that of other regional macro-units on both sides of the South Atlantic, *i.e.,* ancient crystalline basement and metasedimentary units metamorphosed in the Neoproterozoic. In fact, there are significant similarities between the signatures of these regional units in the Kaoko and Dom Feliciano belts. For example, there is a patchy overlap between the metasedimentary rocks of the Damara Supergroup and of the Brusque Group in the Dom Feliciano Belt. On the other hand, the isotopic signatures of the oldest basement fragment in the northern Dom Feliciano Belt, the Camboriú Complex, have similarities with the Archean units that predominate in the Central Kaoko Zone (see Fig. 5). This is in accordance with the proposal that various basement fragments distributed along the extension of the Dom Feliciano have a common origin with the Angola Block of the Congo Craton (Hueck et al., 2022). The regional tectonic implications that can be derived from these observations will be expanded in the following sections.

Having further established the comparison between the Neoproterozoic granitoids of the Kaoko Belt and the Florianópolis Batholith, the discussion can shift towards the implications of the new and compiled dataset, using the extensive literature on the granitic magmatism of the Dom Feliciano Belt (and in particular the Florianópolis Batholith) as an additional framing perspective.

5.2. Magmatic sources: Crust vs. Mantle

The relative contribution of mantle- and crust-derived material in the sources of intermediate to acid magmas and their consequence for the long-term accretion of juvenile material to the continental crust is a topic of significant debate (*e.g.,* Moyen et al., 2017; Jacob et al., 2021 and references therein). The isotopic signatures of the granitoids from the Kaoko Belt, in particular of the Sm-Nd and Rb-Sr systems, which have a strong predominance of values indicative of the reworking of old continental crust, have long been interpreted as an indication that formation of these granitoids was predominantly controlled by the partial melting of crustal sources (Seth et al., 2002; Masberg et al., 2005; Jung et al., 2009; Janoušek et al., 2010, 2023). By itself, however, the predominance of such isotopic signatures with crustal affinities does not necessarily imply in a predominance of crustal sources for the origin of magmatic associations, as crustal contamination is very efficient in overprinting the signatures of mixed mantle-crust magmas and of the subduction-metasomatized asthenosphere (Couzinié et al., 2016; Moyen et al., 2017; Lino et al., 2023), due to the incompatible nature of the trace elements involved in these analyses. For example, Jacob et al. (2021) highlight that even if the bulk mass of a granite originates overwhelmingly from the mantle, its Hf isotopic signature will essentially be controlled by the subordinate crustal contamination, if the mantle source is depleted and the magma experiences significant fractional crystallization. Conversely, Ducea et al. (2015) estimates that at least 50 % of the isotopic signature of magmatic arcs is controlled by the upper plate.

In order to reconstruct potential "hidden" mantle-derived inputs that are most susceptible to crustal contamination (not to mention intrinsic processes such as fractional crystallization), it is useful to also consider minor basic units associated with the more voluminous intermediate to felsic rocks. The traditional interpretation is that these associations are the result of mechanical mingling of basic magma (typically interpreted as a mantle-sourced) that interacted with the main acid magmas, and that the ultimate composition of the granitoid is a result of mixing both magmatic end-members (*e.g.,* Didier & Barbarin, 1991; Barbarin, 2005; Perugini & Poli, 2012). The dataset compiled here includes restricted basic-intermediate rocks (gabbro to diorite) associated with the granitoids, mostly in the form of enclaves (Janoušek et al., 2010, 2023, as well as individual samples in this study) or restricted intrusions (Jung et al., 2009). These samples have clear compositional affinities, particular in their major-element signatures, in which they constitute a well-defined group of basic-intermediate samples in most diagrams (Fig. 3). This affinity, however, does not extend uniformly to their isotopic composition. On the one hand, the samples with isotopic signatures with highest mantle affinity (*i.e.*, more radiogenic Nd-Hf and less radiogenic Sr compositions) and least differentiated geochemical characteristics within the Pan-African magmatic suite come from mafic enclaves hosted within the megacrystic granites of the Amspoort Suite and within the Angra Fria Magmatic Complex within the Coastal terrane, which were interpreted by Janoušek et al., (2010, 2023) as minor inputs of CHUR-like mantle sources. In the case of the former, the authors downplay the significance of mixing of such magmas in the petrogenesis of the igneous association, due to its bimodal nature. On the other hand, restricted quartz-diorite intrusions investigated by Jung et al., (2009) have isotope ratios that widely overlap with nearby differentiated associations, and were therefore interpreted by these authors to be the result of melting of Pan-African metabasaltic source rocks in the lower crust. Similarly conflicting observations have also been made in South America, where the predominance of more "primitive" elemental signatures coming from units associated with the presence of subordinate mafic rock types in the Florianópolis Batholith is commonly interpreted as indicative of important mantle-sourced input that persisted for tens of Myr (Bitencourt et al., 2008, Florisbal et al., 2009, 2012b). However, few of these assumed mantle affinities in South America have been confirmed by direct isotopic evidence, and it is notable that a more detailed U-Pb-Hf investigation of zircon crystals from mafic magmatic enclaves associated with some of the earliest units of the Florianópolis Batholith yielded Lu-Hf signatures that are in fact less radiogenic than that of the more acid granitoids by which they are hosted (Basei et al., 2021). This observation led the authors to suggest scenarios alternative to that of a basic mantle-derived magmatic input to the formation of the enclaves, such as autoliths or the episodic mingling of magmas with similar compositions over a long period of time.

Considering that the evidence above is inconclusive, it is necessary to consider the comparative shift in isotopic affinities of the investigated magmatism relative to other regional units. The fact that the isotopic signatures of the Kaoko Belt granitoids are considerably "less crustal" than those of the basement rocks of the Kaoko Belt has long been interpreted as indicating that the former are not the result of direct partial melting of the latter (Masberg et al., 2005; Janoušek et al., 2010, 2023). In comparison, there is much more significant overlap between the isotopic compositions of the granitoids with that of the metasedimentary sequences of the Kaoko Belt, though the latter often have signatures that extend much farther into "crust-like" values (Figs. 5, 6). While the petrographic and geochemical signatures of the granitoids make it very unlikely that they are predominantly derived from the melting of metasedimentary sources (see section 5.3), it is possible that part of the "mantle-like" isotopic budget of the granitoids may have been derived from these associations.

In order to better compare the isotopic signatures of units with contrasting geological ages, which is not ideal in the diagram of Fig. 5, Fig. 9A presents a Nd evolution diagram following de Paolo (1981), in which the different units are plotted according to their geological age as

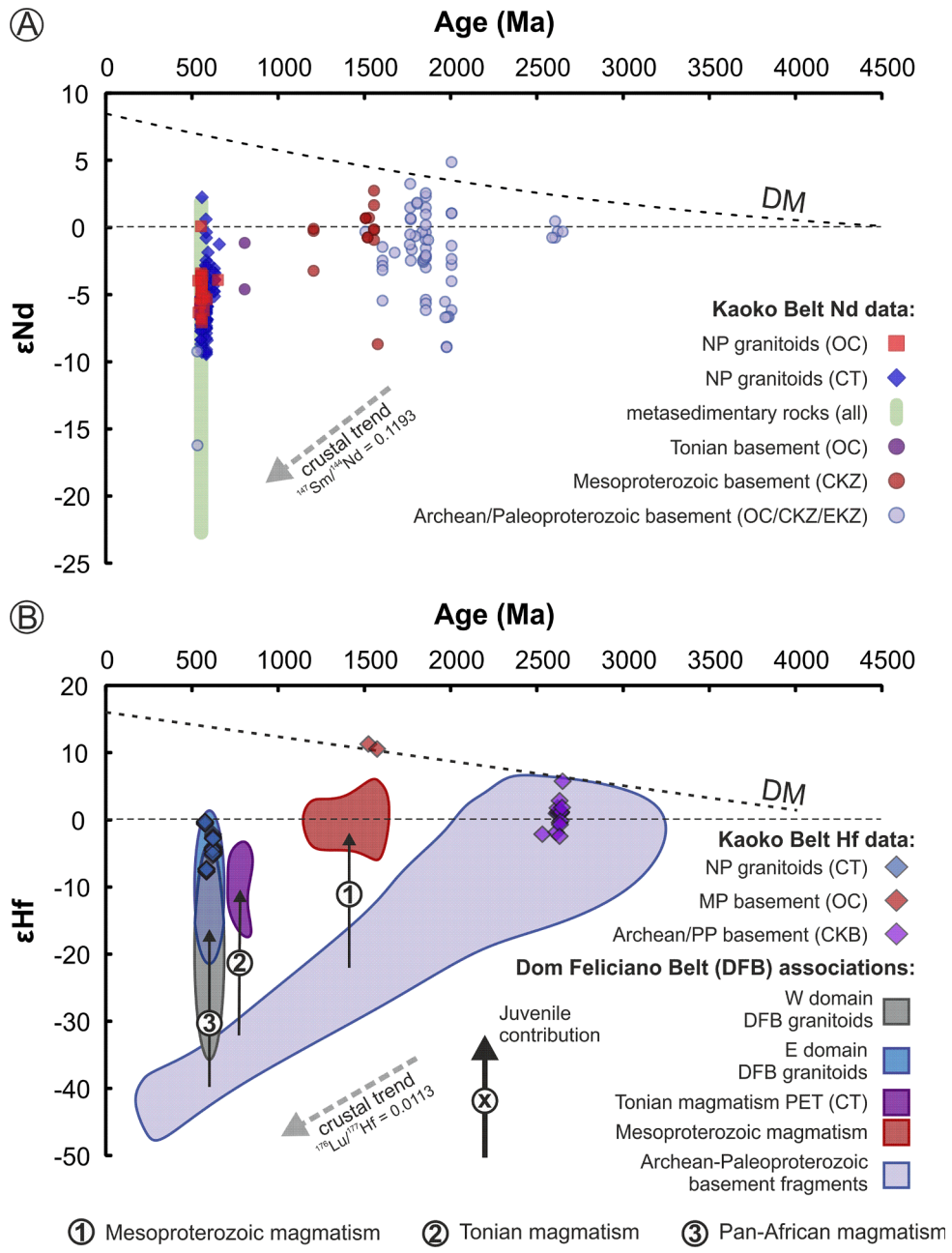

Fig. 9. Sm-Hf isotopic evolution of the Kaoko Belt. A: εNd ratios for whole-rock samples from the Kaoko Belt, plotted according to their age and color-coded according to age and Nd T_{DM} affinities. Note that samples interpreted to have experienced strong crustal reworking are plotted according to the latter age, and that we assume a regional reference age of 550 Ma for metasedimentary rocks; B: published Lu-Hf zircon data for the Kaoko Belt, plotted over a schematic representation of the evolution of Hf signatures compiled for the Dom Feliciano Belt (DFB) and associated units in South America (modified from Hueck et al., 2022). See the text for the sources of the isotopic data from the Kaoko Belt and Hueck et al. (2022) for the sources of the Lu-Hf zircon data compiled for the Dom Feliciano Belt. EKZ/CKZ – Eastern/Central Kaoko Zone, OC – Orogen Core, CT – Coastal Terrane, PET: Punta del Este Terrane (part of the Dom Feliciano Belt), which correlates with the Coastal Terrane of the Kaoko Belt. Average upper crust isotopic compositions are from Taylor & McLennan (1985) and Chauvel et al. (2014).

determined by U-Pb in the same sample or in comparable samples in the literature. In the case of the metasedimentary rocks, which do not have unique crystallization ages, the data is plotted assuming the regional age of 550 Ma used for reference on other isotopic diagrams (Figs. 5 and 6). This diagram is inspired by a similar plot of Lu-Hf data from zircons compiled for granitoids and associated basement domains of the Dom Feliciano Basement in South America (Hueck et al., 2022, Fig. 9B). While a similar compilation is not possible for the Kaoko Belt, because a consistent Lu-Hf dataset representative of all major geological associations there has not been established yet, the few available data (Jung et al., 2012; Konopásek et al., 2016; Oriolo et al., 2016b) are consistent with the Lu-Hf evolution of the Dom Feliciano Belt (Fig. 9B). In addition, considering the similarities between the magmatism on both sides of the Atlantic (section 5.1), the Lu-Hf plot offers a useful point of comparison, because it has the advantage of having a much larger coverage of the diagram, as it includes data from individual crystals that may represent subordinate populations in the analyzed samples (*i.e.,* inherited cores or recent overgrowths). In any case, both diagrams in Fig. 9 indicate that the main basement associations in both belts are dominated by rocks with Archean to Paleoproterozoic model ages, though in the Kaoko Belt there is a significant presence of juvenile material in the late Paleoproterozoic, which is not present in South America. Assuming that these

basement associations are correlated, as has been speculated upon by many authors (Oyhantçabal et al., 2011, 2018; Rapela et al., 2011; Oriolo et al., 2016b, 2019; Basei et al., 2018; Konopásek et al., 2018, 2020; Percival et al., 2021; Hueck et al., 2022), this period would correspond to the assembly of a complex basement association within the Congo-São Francisco paleocontinent, which would have stayed more or less undisturbed except for intra-plate magmatism until the early Neoproterozoic. In this context, Hueck et al. (2022) suggests that at least three different shifts in the U-Pb-Hf zircon dataset in South America seem to correspond to discrete periods of juvenile input in the Mesoproterozoic, Tonian and Ediacaran, modifying the dominant crustal signature of the region (Fig. 9B). This evolutionary trend, also observed in several other orogens throughout Gondwana (*e.g.,* Oriolo et al., 2017; Ganade et al., 2021), seems to be corroborated by the Nd isotopic evolution of the Kaoko Belt (Fig. 9A), and is in accordance with the limited Hf isotope data (Jung et al., 2012; Konopásek et al., 2016; Oriolo et al., 2016b). Even in this framework, the magnitude of the shift in the relative signatures of the Pan-African granitoids suggest an important assimilation of post-Paleoproterozoic juvenile material. The mechanism through which the "mantle-like" isotopic budget was perpetuated into the granitoids is likely a combination between the influence of more radiogenic metasedimentary source rocks and one or more mixtures between mantle-sourced magma with autochthonous crustal melting.

To test the feasibility of the latter scenario of mixing between mantle-derived melts and crustal anatexis sourced from the ancient basement of the Kaoko Belt, Fig. 10 presents mass-balance models of isotopic signatures aimed at exploring the amount of juvenile material needed to achieve the isotopic shifts described above, based on the equations presented by DePaolo and Wasserburg (1979). The input parameters used for modelling and the resulting calculated values are presented in the Supplementary Material G. Using the $^{87}Sr/^{86}Sr_{(550)}$ vs. $\varepsilon_{Nd(550)}$ scheme of Fig. 5 as a basis, Fig. 10A simulates mixing lines between different crustal compositions and mantle-derived end-members. The crustal components consider isotopic ratios from the data compiled for the basement of the belt and average upper-crust elemental compositions (Rudnick & Gao, 2003). The mantle-derived end-member considers an E-MORB elemental composition (Sun & McDonough, 1989;) and depleted mantle (DM) isotopic ratios (de Paolo, 1981; Chauvel & Blichert-Toft, 2001), representing a mantle-derived basaltic composition extracted from a moderately enriched mantle source. An enriched mantle source is likely in this case, considering that the complex association of varied Archean to Paleoproterozoic basement fragments of the Kaoko Belt indicates a protracted collisional assembly and, consequently, an enrichment of its lithospheric mantle, but DM isotopic ratios are used because it is not advisable to extrapolate through time the isotopic values of the more localized E-MORB reservoir. The model assumes equivalent partial melt proportions of both sources for simplicity. As illustrated in Fig. 10A, a mixture starting from the mean and median basement compositions would require an input of *ca.* 70–75 % of mantle-derived magma to achieve an isotopic signature equivalent to the median granitoid composition. While this value seems to confirm the supposition that an important mantle-derived source was involved in the generation of the granitoids, the participation of mantle sources in these results seems somewhat too elevated, considering key geochemical features such as the high K_2O content and the moderately high alumina saturation index. Of course, the results could be refined by changing some of the assumptions in this simplified model, leading to variations in the results. For example, the inclusion of the metasedimentary rocks of the Kaoko Belt as possible crustal source rocks would result in a reduction of the mantle-derived component necessary for achieving isotopic signatures typical of the granitoids. On the other hand, variations in the relative proportion of partial melting of the mantle/crust sources would change the contents in Sr-Nd-Hf of the primary mantle melt relative to the crust, thus modifying the mixing proportion required to get the observed isotopic shifts. Because of the incompatible nature of the elements involved in the models and their considerable higher abundance in crustal rocks compared to the mantle, this would likely imply in a more significant contribution of mantle material to the isotopic budget of the mixture. Also, assuming a less depleted mantle-derived source would also necessitate higher proportions of juvenile material in the mixture. That said, because the wide-ranging and inclusive character of the compiled dataset can lead to the conflating of different magmatic associations (as discussed above), we choose not to over-refine the modelling, highlighting instead its exploratory character.

Another important limit of this model is that it considers a single mantle-derived input at 550 Ma, which is probably an over-simplification, as indicated by the compiled time-integrated isotope data of the Kaoko Belt (Fig. 9). To expand upon this scenario, Fig. 10B illustrates how a similar shift of Nd isotope signatures as the one described above can be achieved by a combination of successive juvenile accretion events. In this figure, *trajectory I* summarizes a scenario similar to the one illustrated in Fig. 10A, that is, in which the mean isotopic signature of the Kaoko basement evolves from its original Archean-Paleoproterozoic signature considering an average upper crust $^{147}Sm/^{144}Nd$ ratio of 0.1193 (Chauvel et al., 2014) until 550 Ma, when it is mixed with the mantle-derived end-member, which in this case requires a juvenile of *ca.* 60–65 % to achieve mean granitoid compositions, which is somewhat below to that of the model in Fig. 10A. Alternatively, *trajectory II* distributes the necessary mantle-sourced input to cause this shift in three consecutive mixing events, after which the isotopic signature of the resulting mixture continues to evolve over time, following the new mean crustal composition. In this illustrative solution, the isotopic shift observed in the compilation is achieved by combining a mixing of *ca.* 40–45 % mantle-derived material in the Mesoproterozoic (1,500 Ma), followed by an addition of *ca.* 30 % juvenile material in the Tonian (800 Ma), and finally an accretion of other 40 to 45 % of mantle-derived basaltic sources in the Ediacaran (550 Ma). Once more, this model follows simplified assumptions, and it is possible that the nature of mantle-derived material varies over time between different accretionary events. This could imply in significant changes in the mantle contribution if less radiogenic isotope ratios are assumed for the mantle-derived end-member. In any case, the results from the models suggest that it is likely that the relatively more radiogenic Nd-Hf signatures of the granitic magmatism in the Kaoko Belt compared to its Archean and Paleoproterozoic basement are the result of significant juvenile input after the Paleoproterozoic, leading to intermediate isotopic signatures (*e.g.,* Arndt and Goldstein, 1987; Jacob et al., 2021).

5.3. Crustal diversity in the Kaoko Belt tracked by its Neoproterozoic magmatism

Assuming, as discussed above, that crustal sources played a role in the genesis of the Pan-African magmatism of the Kaoko Belt, the geochemical and isotopic diversity of the compiled dataset can be used as tracers for the lithological variety of magmatic sources within the belt, and its tectonic organization into different domains. Various possible crustal sources have been suggested for these granitoids in the literature. In a detailed petrogenetic evaluation of the megacrystic Amspoort Suite, the most conspicuous unit of the Border Igneous Complex in the Orogen Core, Janoušek et al. (2010) suggested crustal sources with a predominance of metapsammites with minor metaigneous contribution. More recently, Janoušek et al. (2023) proposed a model of fluid-present partial melting of igneous rocks ranging from basaltic to tonalitic in composition and fluid-absent melting of intermediate to acid rocks, with subordinate influence of metapsammites, for the protracted generation of the Angra Fria Magmatic Complex in the northern portion of the Coastal Terrane. To the south of the Coastal Terrane, Jung et al. (2009) suggested the partial melting of medium-K basalt to explain quartz diorite and granodiorite of the Torrabaai-Koigabmond Complex, and a dominance of metapsammites (possibly from the so-called Nk Formation of the Damara Supergroup, see Jung

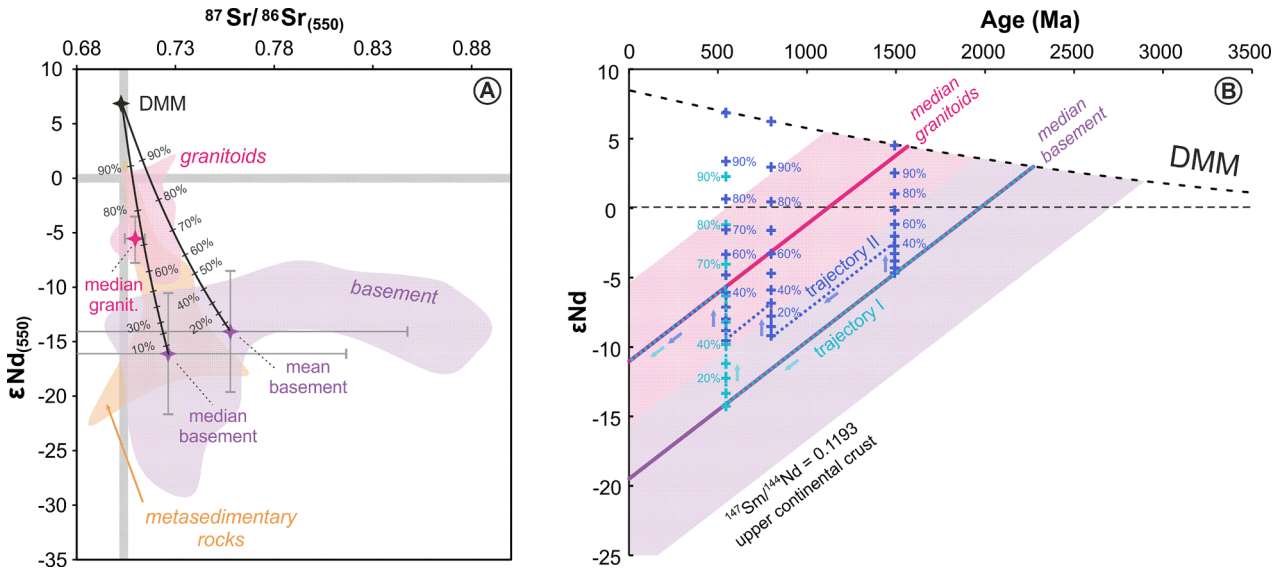

Fig. 10. Mass-balance modelling of isotope signatures simulating the shift of whole-rock signatures of granitoids of the Kaoko Belt relative to its basement due to mixing of a DM/E-MORB mantle-derived end-member (DMM) with partial melting of autochthonous basement rocks. A: $^{87}Sr/^{86}Sr_{(550)}$ vs. $\varepsilon_{Nd(550)}$ diagram with two mixture lines corresponding to mean and median values as starting materials for basement melts; B: ε_{Nd} vs. time diagram, illustrating two possible trajectories that can lead to equivalent shifts of Nd isotope signatures, one with a single mixing at 550 Ma (shown in green), and one with three successive mixings at 1,500, 800, and 550 Ma (shown in blue). See text for further details and Supplementary Material G for the input parameters used for modelling and numerical results. (For interpretation of the references to color in this figure legend, the reader is referred to the web version of this article.)

et al. (2009)) as source of leucogranite in the same unit. In the same region, the so-called Nk granitic pluton is suggested to have been derived from anatexis of intermediate magmatic and metapsammitic sources (Masberg et al., 2005).

In order to assess these hypotheses and test the compiled dataset for possible source rocks, we compare it to compositions from melts

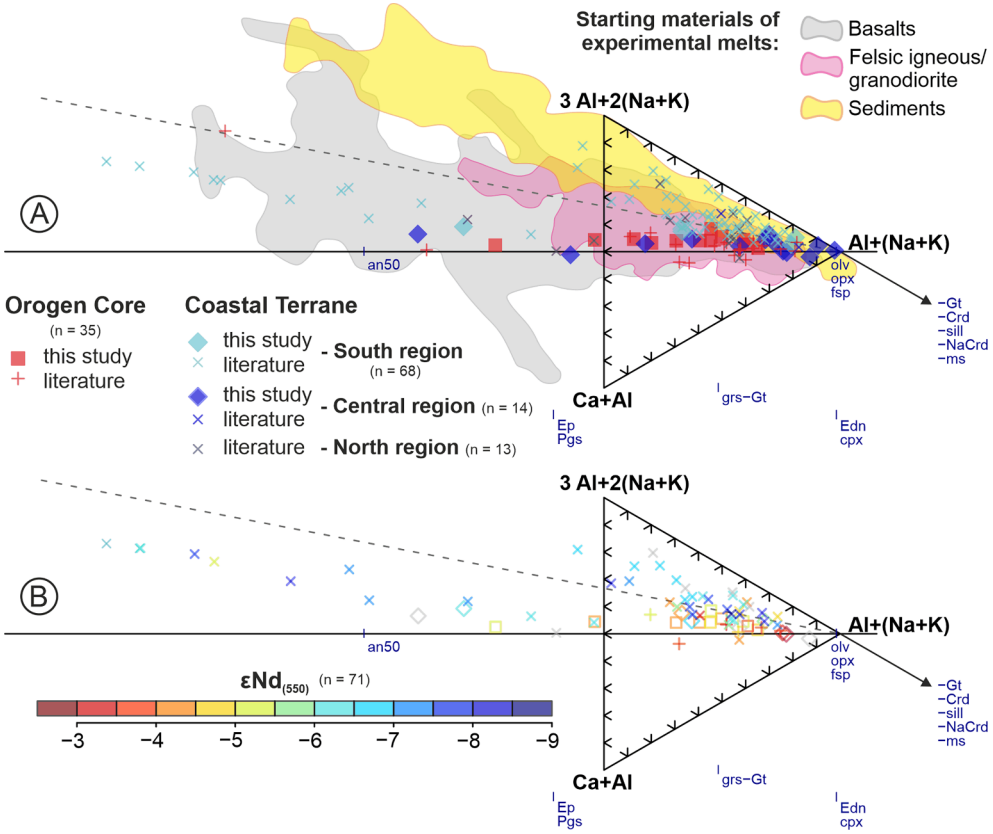

Fig. 11. Whole-rock geochemistry-based source diagram for the Pan-African magmatism in the Kaoko Belt - granitoid compositions projected from biotite onto the Ca + Al − 3Al + 2(Na + K) − Al + (Na + K) plane, with indication of fields defined by experimental results compiled by Moyen et al. (2017). A: samples separated by tectonic domain. B: samples color-coded according to their $\varepsilon_{Nd(550)}$ value. See text for the origin of data compiled from the literature.

produced experimentally from diverse starting materials, using the diagram projecting the granitoid compositions from biotite onto the Ca + Al/3Al + 2(Na + K)/Al + (Na + K) plane (Fig. 11), proposed by Moyen et al. (2017). Only compositions with SiO_2 values > 62 % wt. are plotted in this projection in order to maintain the same compositional range as for the experimental dataset compiled by the same authors, and because the projection is less suited for more basic compositions. Also, while this diagram does not account for the input of mantle-sourced magmas (which is a very reasonable possibility in the studied magmatism, see section 5.2), such a contribution, modified through assimilation and fractional crystallization, should result in compositions plotting in the field of melts derived from basalts, as it would represent a geochemical evolution analogous to the recycling of (mantle-derived) basaltic sources. In this plot, most samples converge towards the Al + (Na + K) vertex of the ternary system, which corresponds to the granitic minimum composition, from which the main trends radiate. When compared to the experimental dataset assembled by Moyen et al. (2017), the field corresponding to compositions associated with sedimentary sources is mostly represented by samples from the southern and, to a lesser degree, northern portions of the Coastal Terrane (Fig. 11A), which is in accordance with a slight predominance of peraluminous compositions in these rocks (Fig. 3F). Elsewhere, most samples fall along trends corresponding to compositions that plot below the dashed line corresponding to a ratio of 2:1 between the 3 Al + 2 (Na + K) and the (Ca + Al) vertexes, which separates more mafic from more felsic sources. This includes trends associated with all tectonic settings, *i.e.,* the Orogen Core and the three sub-regions of the Coastal Terrane. Such discriminations are less useful towards the Al + (Na + K) vertex of the ternary system, in which there is a large overlap of experimental melts resulting from different starting materials due to its affinity with eutectic compositions.

The observations above can further be compared with Sm-Nd isotopic signatures from samples for which this data is available (Fig. 11B). In this diagram, the more radiogenic compositions tend to concentrate closer to the Al + (Na + K) vertex, whereas $\varepsilon_{Nd(550)}$ values indicative of a stronger influence of old crustal sources mostly spread along the main trends plotting outwards of the ternary diagram. Interestingly, this includes both the trend plotting over the field associated with sedimentary sources as well as the one comprising samples that plot over the field associated with basaltic starting compositions. Both trends are especially prevalent in samples from the southern portion of the Coastal Terrane, which reflects the comparatively less radiogenic $\varepsilon_{Nd(550)}$ values of this region in general (Fig. 5B). In fact, this prevalence of less radiogenic signatures within the southern portion of the Coastal Terrane, together with the major-element signatures compatible with the incorporation of metasedimentary rocks in its magmatic sources in the same region, is the clearest set of characteristics that separates any group of granitoids from another in the compilation. Considering that the samples that, in this diagram, have the most affinity with metasedimentary sources are not characterized by more juvenile Nd signatures as would be expected from Fig. 5, it is possible that the influence of the incorporation of metasedimentary material in the crustal sources of the magmatism did not have a major impact in the resulting isotopic signatures. In contrast, the other major subdivision of granitoids have overall very similar signatures, reflecting the observations also applied to the geochemical dataset in general (Figs. 3, 4). The compositional similarities of coeval rocks from the two main sub-division of the Western Kaoko Zone, namely the Orogen Core and the Coastal Terrane, is suggestive of at least a partial equivalence between the crustal units involved in the genesis of the Pan-African magmatic in both terranes, and disagrees with the idea of a sharp terrane boundary between them (*e.g.,* Goscombe & Gray, 2008, see section 5.4).

5.4. *Tectonic architecture of the Kaoko Belt in the context of the South Atlantic Pan-African systems*

The tectonic evolution of the Kaoko Belt and of its South American counterpart, the Dom Feliciano Belt, has traditionally been interpreted in terms of an accretionary orogen followed by continental collision (*e.g.,* Basei et al., 2000, 2005, 2008, 2018; Goscombe & Gray, 2007,2008; Konopásek et al., 2008; Oyhantçabal et al., 2009; Saalmann et al., 2011; Frimmel et al., 2011; Oriolo et al., 2016a; Passchier et al., 2016; Philipp et al., 2016; Goscombe et al., 2017; Frimmel, 2018; Hueck et al., 2019; Will et al., 2019, 2020). In this configuration, the Coastal Terrane and the Florianópolis Batholith in the Dom Feliciano Belt originally would have evolved as a magmatic arc outboard and to the west of the rest of the Kaoko Belt, as consequence of eastward subduction of the Adamastor oceanic lithosphere. Only later, with the thrusting of the Coastal Terrane over the Kaoko Belt proper at *ca.* 590–580 Ma, would the rest of the Belt have experienced regional metamorphism and deformation, until *ca.* 550 Ma. Some recent versions of this model (*e.g.,* Hueck et al., 2019), from a South American perspective, estimate that the collision to the west of the Coastal Terrane took place at *ca.* 615 Ma. This would mean that remnants of the arc stage (>615 Ma) are relatively underrepresented on both sides of the Atlantic, because of the overall low long-term preservation potential of arc rocks (*e.g.,* Hawkesworth et al., 2010).

More recently, an alternative view proposes that closure of an intracontinental basin without subduction (of Adamastor oceanic lithosphere) would explain the Kaoko Belt (Konopásek et al., 2018, 2020; Fossen et al., 2020; Percival et al., 2021, 2022; Janoušek et al., 2023). These authors suggest that continental extension and rifting in the Tonian without developing into a drifting stage would give rise to the rift basin in which sediments that are now found as metasedimentary cover rocks in all orogenic associations in the system were deposited. Deformation, metamorphism and intrusion of abundant granitic magmas then took place when extension was inverted to compression, leading to successive convergence of the main crustal segments.

To address the conflicting models, it is useful to consider the integrated isotopic architecture of the Kaoko and Dom Feliciano belts, and its implications for the relative contribution of crustal and mantle sources for the origins of the investigated Pan-African magmatism, as discussed in sections 5.2 and 5.3. The shift in isotopic signatures suggestive of a post-Paleoproterozoic juvenile input discussed above for the Kaoko Belt is also observed in the western domain of the Dom Feliciano Belt (*i.e.,* Florianópolis Batholith and its basement within the Punta del Este Terrane, see Fig. 8B and 9B), constituting a well-characterized isotopic boundary within the belt, the Major Gercino-Sierra Ballena lineament (*e.g.,* Basei et al., 2000; Hueck et al., 2018, 2019, 2020a; Lara et al., 2021 and references therein). The resulting configuration is that of an isotopically "young" crustal segment (Coastal Terrane/Florianópolis Batholith/Punta del Este Terrane) that is surrounded on both sides by ancient basement with dominantly Archean signatures. As discussed in section 5.2, based on the available isotopic evidence (Fig. 9) and the modelling presented in this manuscript, this requires a significant juvenile input at some point after the assembly of most of the basement terranes in the Paleoproterozoic.

One straightforward solution for this input could be the impact of juvenile accretion during the formation of an Ediacaran continental arc along the western margin of the Kaoko Belt, in the subduction-based tectonic model mentioned above (*e.g.,* Basei et al., 2000, 2005, 2008, 2018; Goscombe & Gray, 2007,2008). This model proposes Eastwards-dipping subduction of the Adamastor Ocean below the western margin of the Angola Block, with the ultimate suture corresponding to the present-day Major Gercino-Sierra Ballena Lineament in South America. Because this model proposes that both the Coastal Terrane and the Orogen Core of the Kaoko Belt would have been developed in the same tectonic context (*i.e.,* the upper plate, with a continental arc until *ca.* 615 Ma), it is in agreement with the similarities reported here for the geochemical and isotope signatures of the granitoids hosted in both terranes. The main differences between them, particularly the predominance of older intrusion ages in the Coastal Terrane, would be the result of the juxtaposition of the latter over the rest of Kaoko Belt occurring only later, at *ca.* 590–580 Ma, consequently leading to regional

metamorphism and abundant magmatic activity (*e.g.,* Goscombe et al., 2005a, 2017). The fact that the vast majority of the granitoids currently exposed were emplaced subsequently to the actual timing of the collision along the subduction front (*ca.* 615 Ma, see above) is not in contradiction with this model, as the syn-and post-collisional recycling of the magmatism after the establishment of an arc system would only perpetuate the isotopic signature of this source in the following granitoids (Ducea et al., 2015), but with a much higher potential for preservation (Hawkesworth et al., 2010).

On the other hand, there are noteworthy evidences that key characteristics of the Ediacaran granitoids from the entire Dom Feliciano Belt, including their isotopic signatures, are shared with their immediate basement, and are thus likely to have been inherited through the partial melting of crustal sources (Florisbal et al., 2012a; Hueck et al., 2016, 2020a; Lara et al., 2017, 2020, 2021). In this context, it is possible that some or much of the juvenile input deduced in the area took place prior to the main Pan-African orogenic cycle (*i.e.,* before 650 Ma, see Fig. 10B). The most likely candidates for such an event would be in the Mesoproterozoic, of which there are remnants in both belts (*e.g.,* Jung et al., 2012), and in the Tonian. The latter is associated with the crystallization of restricted 800–750 Ma protoliths of orthogneisses exposed mostly in the Coastal Terrane and subordinately in the Orogen Core of the Kaoko Belt, but with much larger exposures in the Dom Feliciano Belt (see review in Hueck et al., 2022). This magmatism has been alternatively interpreted as a magmatic arc (Masquelin et al., 2012; Lenz et al., 2011; Koester et al., 2016; Ramos et al., 2018, 2020; de Toni et al., 2020) or as rifting-related granites with abundant crustal assimilation (Basei et al., 2008, 2011a, 2018; Konopásek et al., 2018, 2020; Will et al., 2019, 2020). Ultimately, it cannot be discarded that the juvenile input associated with this event might be responsible for much of the rejuvenated isotopic signature of the Kaoko granitoids (Fig. 10B). Thus, it could accommodate an Ediacaran genesis unrelated to subduction and dominated by crustal melting as proposed by Janoušek et al. (2023), though involving sources previously modified in the Tonian, instead of a juvenile Eburnean (*i.e.,* Paleoproterozoic) crust suggested by these authors. It is notable, however, that the Ediacaran Nd-Hf signatures from the Kaoko granitoids and from its correspondents in the Dom Feliciano Belt can have more radiogenic signatures than those of their immediate basement (Fig. 9B).

Finally, the discussion above also has implications for the tectonic significance of the main shear zones of the Kaoko Belt. While the role of shear zones during the evolution of the orogeny has been highlighted in numerous past studies, there is disagreement in the literature on whether they represent early terrane boundaries separating different crustal blocks from the initial stages of regional deformation and metamorphism onwards (Goscombe & Gray, 2008; Foster et al., 2009), or are alternatively the result of strain localization during the late stages of the orogeny following the transition from transpressive to transcurrent deformation (Konopásek et al., 2005; Ulrich et al., 2011). The strong contrast between the signatures from the Kaoko granitoids and the Archean to Paleoproterozoic basement in the Eastern and Central Kaoko Zones, together with the seemingly analogous isotopic architecture of the Dom Feliciano Belt, suggest that there could be a significant isotopic boundary in the orogenic system. Such a prominent contrast could be interpreted as evidence of an early (pre-orogenic) terrane border in the sense of, *e.g.,* Goscombe & Gray (2008). Based on the exotic characteristics of the Coastal Terrane, it would be tempting to associate this limit with its eastern border, *i.e.,* the Three Palms Shear Zone (Goscombe & Gray, 2007; Oriolo et al., 2018). However, this shear zone is characterized by a wide network of transpressive sinistral belts branching out and connecting to one another, along which rocks associated both with the Coastal Terrane and the Orogen Core became juxtaposed. Konopásek et al. (2008,2014) considered the easternmost branch of the Three Palms Shear Zone, known as the Village Mylonitic Zone, the eastern limit of the Coastal Terrane, as it approximately corresponds to the easternmost aerial extent of the intrusive Neoproterozoic magmatic rocks. However, in addition to the extent of Neoproterozoic magmatism, there are other characteristics, such as the presence of Mesoproterozoic basement and relative lack of Archean associations, that distinguish the Orogen Core (and the West Kaoko Zone in general) from the rest of the Kaoko Belt. On the other hand, the main connection between the Orogen Core and the Central and Eastern Kaoko zones resides in similarities between their metasedimentary units (*e.g.,* Konopásek et al., 2014). However, the isotopic signatures of these units are effectively controlled by their sedimentary sources, and they may well have been deposited after the establishment of the initial precursor to the present-day isotopic boundary in the Tonian. For these reasons, if there is an early terrane boundary in the Kaoko Belt, the limit between the Western and Central Kaoko zones, *i.e.,* the Puros Shear Zone, may be a more credible candidate for it. This suggestion is compatible with the configuration of the structure, which is the sharpest structural lineament of the Kaoko Belt, with a mylonitic zone up to 5 km wide (Konopásek et al., 2005; Goscombe & Gray, 2008; Ulrich et al., 2011).

6. Conclusions

A comprehensive evaluation of Neoproterozoic plutonic rocks in the Kaoko Belt reveals valuable information on the evolution and tectonic organization of the belt during the Pan-African orogenic cycle. The extensive new dataset strengthens previous trans-Atlantic correlations between this granitic association and the coeval Florianópolis Batholith, one of the main units of the Dom Feliciano Belt in South America. The new U-Pb ages highlight how both granitic manifestations have two main pulses of magmatic activity at *ca.* 620–610 and 590–580 Ma. An apparent gap in pooled ages between *ca.* 610 and 595 Ma, exclusive to the Kaoko Belt, is still represented by individual zircon crystals preserved in younger intrusions. The migration of the orogenic front from (present-day) South America towards Africa means that the Kaoko Belt experienced extensive magmatism between *ca.* 580 and 550 Ma, whereas in South America this period corresponds to a gradual decrease in orogenic activity. Whole-rock elemental and isotopic geochemical data does not reveal major differences in the compositional range of granitoids from different domains of the Western Kaoko Belt, namely between rocks intrusive into the Orogen Core and into the Coastal Terrane, or between subdivisions of the latter. This suggests that the entire Western Kaoko Zone comprises a diverse set of similar geologic units that were likely tapped recurrently during magmatic activity in the Neoproterozoic. On the other hand, while the isotope signatures of the Pan-African magmatism of the Kaoko Belt have a predominantly crustal affinity, it is markedly more juvenile than the signatures of most basement associations and many metasedimentary sequences of the Kaoko Belt. This configuration corresponds to a mirror image of the tectonic situation of South America, in which an isotopic boundary separates the Dom Feliciano Belt into a western domain dominated by Archean to Paleoproterozoic isotopic signatures and an eastern domain that is very similar to the Coastal Terrane of the Kaoko Belt. This observation could reflect a tectonic boundary within the Kaoko Belt that may have acted as an early terrane border during the belt's evolution, essentially contrasting the Western Kaoko Zone from the remaining domains of the belt in isotopic terms, which could correspond to the Puros Shear Zone. The presence of an isotopically more juvenile basement in the center of the orogenic system defined by both belts implies in a significant input of juvenile material at some point after the Paleoproterozoic, when the pre-Pan-African basement of both belts was probably consolidated. This juvenile input is likely the result of intracontinental Mesoproterozoic magmatism and accretionary orogeny and/or rifting, in the Tonian, in the Ediacaran, or both.

CRediT authorship contribution statement

Mathias Hueck: Writing – review & editing, Writing – original draft, Visualization, Methodology, Formal analysis, Data curation,

Conceptualization. **Miguel A.S. Basei:** Writing – review & editing, Supervision, Project administration, Methodology, Investigation, Funding acquisition, Conceptualization. **Hartwig Frimmel:** Writing – review & editing, Visualization, Resources, Methodology, Investigation. **Lucas M. Lino:** Writing – review & editing, Visualization, Validation, Investigation, Formal analysis. **Vinicius X. Corrêa:** Visualization, Formal analysis, Data curation. **Lucas R. Tesser:** Writing – review & editing, Conceptualization. **Mario C. Campos Neto:** Writing – review & editing, Validation, Supervision. **Carlos E. Ganade:** Writing – review & editing, Validation, Investigation.

Declaration of competing interest

The authors declare that they have no known competing financial interests or personal relationships that could have appeared to influence the work reported in this paper.

Data availability

New data is included in the supplementary materials

Acknowledgements

This work was funded by FAPESP through the Thematic Projects 2005/58688-1 and 2015/03737-0, as well as individual scholarships and fellowships to M.H. (2019/06838-2), L.M.L. (2023/06771-0), and L. R.T (2021/06106-1).We would like to thank the institutional support offered by the Geological Survey of Namibia, and in particular the assistance of Anna K. Nguno. We also thank Jean-Baptiste Jacob and Stefan Jung for their detailed and constructive reviews, and editors Sebastián Oriolo and Wilson Teixeira for the efficient handling of the manuscript.

Appendix A. Supplementary data

Supplementary data to this article can be found online at https://doi.org/10.1016/j.precamres.2024.107366.

References

Annen, C., Blundy, J.D., Leuthold, J., Sparks, R.S.J., 2015. Construction and evolution of igneous bodies: Towards an integrated perspective of crustal magmatism. Lithos 230, 206–221.

Arndt, N.T., Goldstein, S.L., 1987. Use and abuse of crust-formation ages. Geology 15 (10), 893–895.

Barbarin, B., 2005. Mafic magmatic enclaves and mafic rocks associated with some granitoids of the central Sierra Nevada batholith, California: nature, origin, and relations with the hosts. Lithos 80 (1–4), 155–177.

Barboni, M., Schoene, B., Ovtcharova, M., Bussy, F., Schaltegger, U., Gerdes, A., 2013. Timing of incremental pluton construction and magmatic activity in a back-arc setting revealed by ID-TIMS U/Pb and hf isotopes on complex zircon grains. Chem. Geol. 342, 76–93.

Basei, M.A., Corrêa, V.X., Castro, N.A., Hueck, M., 2021. U-pb geochronology and Lu–Hf zircon isotopy of the santinho granitic association: a remnant of the early magmatic stages of the Florianópolis batholith, Santa Catarina, Brazil. J. South Am. Earth Sci. 108, 103148.

Basei, M.A.S., Frimmel, H.E., Nutman, A.P., Preciozzi, F., Jacob, J., 2005. The connection between the neoproterozoic Dom Feliciano (Brazil/Uruguay) and Gariep (Namibia/South Africa) orogenic belts. Precambr. Res. 139, 139–221.

Basei, M.A.S., Frimmel, H.E., Nutman, A.P., Preciozzi, F., 2008. West Gondwana amalgamation based on detrital zircon ages from neoproterozoic Ribeira and Dom Feliciano belts of South America and comparison with coeval sequences from SW Africa. In: Pankhurst, R.J., Trouw, R.A.J., de Brito Neves, B.B., de Wit, M.J. (Eds.), West Gondwana: Pre-Cenozoic Correlations across the Ad South Atlantic Region, 294. Geological Society London, Special Publication, London, pp. 239–256.

Basei, M.A.S., Peel, E., Sánchez Bettucci, L., Preciozzi, F., Nutman, A.P., 2011a. The basement of the Punta del Este terrane (Uruguay): an african mesoproterozoic fragment at the eastern border of the south American río de la Plata craton. International Journa of Earth Sciences 100, 289–304.

Basei, M.A.S., Drukas, C.O., Nutman, A., Wemmer, P.K., Dunyi, L., Santos, P.R., Passarelli, C.R., Campos-Neto, M.C., Siga Jr., O., Osako, L., 2011b. The Itajaí foreland basin: a tectono-sedimentary record of the Ediacaran period, southern Brazil. Int. J. Earth Sci. 100, 543–569.

Basei, M.A.S., Siga Jr., O., Masquelin, H., Harara, O.M., Reis Neto, J.M., Preciozzi, F., 2000. The Dom Feliciano Belt of Brazil and Uruguay and its Foreland Domain the Rio de la Plata Craton: framework, tectonic evolution and correlation with similar provinces of Southwestern Africa. In: Cordani, U.G., Milani, E.J., Thomaz Filho, A., Campos, D.A. (Eds.), Tectonic Evolution of South America, IGC 31, Rio de Janeiro, 311-334.

Basei, M.A.S., Frimmel, H., Campos Neto, M.C., Ganade, C.E., Castro, N.A., Passarelli, C. R., 2018. The tectonic history of the southern Adamastor Ocean based on a Correlation of the kaoko and Dom Feliciano belts. In: Siegesmund, S., Oyhantçabal, P., Basei, M.A.S., Oriolo, S. (Eds.), Geology of Southwest Gondwana. Regional Geology Reviews, Springer, Heidelberg, pp. 63–85.

Bea, F., Montero, P., Barcos, L., Cambeses, A., Molina, J.F., Morales, I., 2023. Understanding nd model ages of granite rocks: the effects of the 147Sm/144Nd variability during partial melting and crystallization. Lithos 436, 106940.

Bitencourt, M.F., Bongiolo, E., Philipp, R.P., Morales, L.F., Ruber, R.R., Melo, C.L., Luft Jr., J.L., 2008. Estratigrafia do batólito Florianópolis, cinturão Dom Feliciano, na região de Garopaba-Paulo Lopes, SC. Pesquisas Em Geociências 35, 109–136.

Boynton, W.V., 1984. Cosmochemistry of the rare earth elements: meteorite studies. Dev. Geochem. 2, 63–114.

Brown, M., 2007. Crustal melting and melt extraction, ascent and emplacement in orogens: mechanisms and consequences. J. Geol. Soc. Lond. 164, 709–730.

Cawood, P.A., Hawkesworth, C.J., Dhuime, B., 2013. The continental record and the generation of continental crust. GSA Bull. 125 (1–2), 14–32.

Chauvel, C., Blichert-Toft, J., 2001. A hafnium isotope and trace element perspective on melting of the depleted mantle. Earth Planet. Sci. Lett. 190 (3–4), 137–151.

Chauvel, C., Garçon, M., Bureau, S., Besnault, A., Jahn, B.M., Ding, Z., 2014. Constraints from loess on the Hf–Nd isotopic composition of the upper continental crust. Earth Planet. Sci. Lett. 388, 48–58.

Chemale Jr, F., Kawashita, K., Dussin, I.A., Ávila, J.N., Justino, D., Bertotti, A., 2012. U-pb zircon in situ dating with LA-MC-ICP-MS using a mixed detector configuration. An. Acad. Bras. Cienc. 84 (2), 275–296.

Corrêa, V. X., 2016. Geoquímica, isotopia e geocronologia das rochas graníticas do Batolito Florianópolis na Ilha de Santa Catarina, SC, Brasil. MSc Dissertation, University of São Paulo.

Couzinié, S., Laurent, O., Moyen, J.F., Zeh, A., Bouilhol, P., Villaros, A., 2016. Post-collisional magmatism: crustal growth not identified by zircon Hf–O isotopes. Earth Planet. Sci. Lett. 456, 182–195.

De Paolo, D.J., 1981. Neodymium isotopes in the Colorado front range and crust-mantle evolution in the proterozoic. Nature 29, 193–196.

De Toni, G.B., Bitencourt, M.F., Nardi, L.V.S., Florisbal, L.M., Almeida, B.S., Geraldes, M., 2020. Dom Feliciano Belt orogenic cycle tracked by its pre-collisional magmatism: the tonian (ca. 800 ma) Porto Belo complex and its correlations in southern Brazil and Uruguay. Precambr. Res. https://doi.org/10.1016/j.precamres.2020.105702.

DePaolo, D.J., Wasserburg, G.J., 1979. Petrogenetic mixing models and nd-sr isotopic patterns. Geochim. Cosmochim. Acta 43 (4), 615–627.

Didier, J., Barbarin, B., 1991. Enclaves and granite Petrology. Developments in petrology 13. Elsevier.

Ducea, M.N., Saleeby, J.B., Bergantz, G., 2015. The architecture, chemistry, and evolution of continental magmatic arcs. Annu. Rev. Earth Planet. Sci. 43, 299–331.

Florisbal, L.M., Bitencourt, M.F., Nardi, L.V.S., Conceição, R.V., 2009. Early postcollisional granitic and coeval mafic magmatism of medium- to high-K tholeiitic affinity within the neoproterozoic southern brazilian Shear Belt. Precambr. Res. 175, 135–148.

Florisbal, L.M., Janasi, V.A., Bitencourt, M.F., Heaman, L.M., 2012a. Space-time relation of post-collisional granitic magmatism in Santa Catarina, southern Brazil: U-pb LAMC-ICP-MS zircon geochronology of coeval mafic-felsic magmatism related to the Major Gercino Shear zone. Precambr. Res. 216–219, 132–151.

Florisbal, L.M., Bitencourt, M.F., Janasi, V.A., Nardi, L.V.S., Heaman, L.M., 2012b. Petrogenesis of syntectonic granites emplaced at the transition from thrusting to transcurrent tectonics in post-collisional setting: whole-rock and sr-nd-pb isotope geochemistry in the neoproterozoic quatro Ilhas and Mariscal granites, southern Brazil. Lithos 153, 53–71.

Florisbal, L.M., Janasi, V.A., Bitencourt, M.F., Nardi, L.V.S., Heaman, L.M., 2012c. Contrasted crustal sources as defined by whole-rock and Sr–Nd–Pb isotope geochemistry of neoproterozoic early post-collisional granitic magmatism within the southern brazilian Shear Belt, Camboriú, Brazil. Journal of South American Earth Science 39, 24–43.

Fossen, H., Cavalcante, C., Konopásek, J., Meira, V.T., Almeida, R.P., Hollanda, M.H.B., Trompette, R., 2020. A critical discussion of the subduction-collision model for the neoproterozoic Araçuaí-West Congo orogen. Precambr. Res. 343 https://doi.org/10.1016/j.precamres.2020.105715.

Foster, D.A., Goscombe, B.D., Gray, D.R., 2009. Rapid exhumation of deep crust in an obliquely convergent orogeny: the Kaoko Belt of the Damara orogen. Tectonics. https://doi.org/10.1029/2008TC002317.

Franz, L., Romer, R.L., Dingeldey, D.P., 1999. Diachronous Pan-african granulite-facies metamorphism (650 ma and 550 ma) in the kaoko belt, NW Namibia. Eur. J. Mineral. 11 (1), 167–180.

Frimmel, H.E., 2018. The Gariep Belt. In: Siegesmund, S., Oyhantçabal, P., Basei, M.A.S., Oriolo, S. (Eds.), Geology of Southwest Gondwana. Regional Geology Reviews, Springer, Heidelberg, pp. 353–386.

Frimmel, H.E., Basei, M.A.S., Gaucher, C., 2011. Neoproterozoic geodynamic evolution of sW–Gondwana: a southern african perspective. Int. J. Earth Sci. 100, 323–354.

Frost, B.R., Barnes, C.G., Collins, W.J., Arculus, R.J., Ellis, D.J., Frost, C.D., 2001. A geochemical classification for granitic rocks. J. Petrol. 42, 2033–2048.

Ganade, C.E., Weinberg, R.F., Caxito, F.A., Lopes, L.B., Tesser, L.R., Costa, I.S., 2021. Decratonization by rifting enables orogenic reworking and transcurrent dispersal of old terranes in NE Brazil. Sci. Rep. 11 (1), 5719.
Gao, P., Wang, Y., Sun, G.C., Mayne, M.J., Zhang, J., Yin, C., Qian, J., 2023. The contributions of (meta-) sedimentary or granitic orthogneissic sources to the cenozoic himalayan granites. Contrib. Miner. Petrol. 178 (7), 1–21.
Gaschnig, R.M., Vervoort, J.D., Lewis, R.S., Tikoff, B., 2013. Probing for proterozoic and archean crust in the northern US cordillera with inherited zircon from the Idaho batholith. GSA Bull. 125 (1–2), 73–88.
Goscombe, B., Gray, D.R., 2007. The coastal terrane of the Kaoko Belt, Namibia: outboard arc-terrane and tectonic significance. Precambr. Res. 155 (1), 139–158.
Goscombe, B., Hand, M., Gray, D., 2003a. Structure of the Kaoko Belt, Namibia: progressive evolution of a classic transpressional orogen. J. Struct. Geol. 25 (7), 1049–1081.
Goscombe, B., Hand, M., Gray, D., Mawby, J., 2003b. The metamorphic architecture of a transpressional orogen: the Kaoko Belt, Namibia. J. Petrol. 44 (4), 679–711.
Goscombe, B., Gray, D., Armstrong, R., Foster, D.A., Vogl, J., 2005b. Event geochronology of the Pan-african Kaoko Belt, Namibia. Precambr. Res. 140, 103. e1–103.e41.
Goscombe, B., Foster, D.R., Gray, D., Wade, B., Marsellos, A., Titus, J., 2017. Deformation correlations, stress field switches and evolution of an orogenic intersection: the Pan-african kaoko-Damara orogenic junction, Namibia. Geosci. Front. 8 (6), 1187–1232.
Goscombe, B., Foster, D.A., Gray, D., Wade, B., 2018. The evolution of the Damara orogenic system: a record of West Gondwana assembly and crustal response. In: Siegesmund, S., Oyhantçabal, P., Basei, M.A.S., Oriolo, S. (Eds.), Geology of Southwest Gondwana. Regional Geology Reviews, Springer, Heidelberg, pp. 303–352.
Goscombe, B.E.N., Gray, D., Hand, M., 2005a. Extrusional tectonics in the core of a transpressional orogen; the Kaoko Belt, Namibia. J. Petrol. 46 (6), 1203–1241.
Goscombe, B., Gray, D.R., 2008. Structure and strain variation at mid-crustal levels in a transpressional orogen: a review of Kaoko Belt structure and the character of West Gondwana amalgamation and dispersal. Gondw. Res. 13 (1), 45–85.
Hawkesworth, C.J., Dhuime, B., Pietranik, A.B., Cawood, P.A., Kemp, A.I., Storey, C.D., 2010. The generation and evolution of the continental crust. J. Geol. Soc. Lond. 167 (2), 229–248.
Hoffman, P.F., Kaufman, A.J., Halverson, G.P., Schrag, D.P., 1998. A neoproterozoic snowball earth. Science 281 (5381), 1342–1346.
Hoffman, P.F., Halverson, G.P., Schrag, D.P., Higgins, J.A., Domack, E.W., Macdonald, F. A., Nelson, L.L., 2021. Snowballs in Africa: sectioning a long-lived neoproterozoic carbonate platform and its bathyal foreslope (NW Namibia). Earth Sci. Rev. 219, 103616.
Hueck, M., Basei, M.A.S., de Castro, N.A., 2016. Origin and evolution of the granitic intrusions in the brusque Group of the Dom Feliciano Belt, south Brazil: petrostructural analysis and whole-rock/isotope geochemistry. J. s. Am. Earth Sci. 69, 131–151.
Hueck, M., Oyhantçabal, P., Philipp, R.P., Basei, M.A.S., Siegesmund, S., 2018. The Dom Feliciano Belt in southern Brazil and Uruguay. In: Siegesmund, S., Oyhantçabal, P., Basei, M.A.S., Oriolo, S. (Eds.), Geology of Southwest Gondwana. Regional Geology Reviews, Springer, Heidelberg, pp. 267–302.
Hueck, M., Basei, M.A.S., Wemmer, K., Oriolo, S., Heidelbach, F., Siegesmund, S., 2019. Evolution of the Major Gercino Shear zone in the Dom Feliciano Belt, South Brazil, and implications for the assembly of southwestern Gondwana. Int. J. Earth Sci. 108, 403–425.
Hueck, M., Basei, M.A.S., de Castro, N.A., 2020a. Tracking the sources and the evolution of the late neoproterozoic granitic intrusions in the brusque group, Dom Feliciano Belt, South Brazil: LA-ICP-MS and SHRIMP geochronology coupled to hf isotopic analysis. Precambr. Res. 338, 105566.
Hueck, M., Wemmer, K., Basei, M.A., Philipp, R.P., Oriolo, S., Heidelbach, F., Oyhantçabal, P., Siegesmund, S., 2020b. Dating recurrent shear zone activity and the transition from ductile to brittle deformation: white mica geochronology applied to the neoproterozoic Dom Feliciano Belt in South Brazil. J. Struct. Geol. 141, 104199.
Hueck, M., Oriolo, S., Basei, M.A., Oyhantçabal, P., Heller, B.M., Wemmer, K., Siegesmund, S., 2022. Archean to early neoproterozoic crustal growth of the southern south American platform and its wide-reaching "african" origins. Precambr. Res. 369, 106532.
Jacob, J.B., Moyen, J.F., Fiannacca, P., Laurent, O., Bachmann, O., Janoušek, V., Villaros, A., 2021. Crustal melting vs. fractionation of basaltic magmas: part 2, attempting to quantify mantle and crustal contributions in granitoids. Lithos 402, 106292.
Janoušek, V., Farrow, C.M., Erban, V., 2006. Interpretation of whole-rock geochemical data in igneous geochemistry: introducing geochemical data toolkit (GCDkit). J. Petrol. 47 (6), 1255–1259.
Janoušek, V., Konopásek, J., Ulrich, S., Erban, V., Tajčmanová, L., Jeřábek, P., 2010. Geochemical character and petrogenesis of Pan-african amspoort suite of the Boundary igneous complex in the Kaoko Belt (NW Namibia). Gondw. Res. 18 (4), 688–707.
Janoušek, V., Moyen, J.F., Martin, H., Erban, V., Farrow, C., 2016. Geochemical modelling of igneous processes: principles and recipes in R language. Springer, Heidelberg, p. 354.
Janoušek, V., Florisbal, L.M., Konopásek, J., Jeřábek, P., Bitencourt, M.F., Gadas, P., Kopačková-Strnadová, V., 2023. Arc-like magmatism in syn-to post-collisional setting: the Ediacaran angra Fria magmatic complex (NW Namibia) and its cross-Atlantic correlatives in the south brazilian Florianópolis batholith. J. Geodyn. 155, 101960.
Jelinek, A.R., Bastos-Neto, A.C., Leite, J.A., Hartmann, L.A., McNaughton, N.J., 2005. SHRIMP U-pb zircon dating of pedras grandes suite, southern Santa Catarina state, Brazil. An. Acad. Bras. Cienc. 77 (1), 125–135.
Jelsma, H.A., McCourt, S., Perritt, S.H., Armstrong, R.A., 2018. The geology and evolution of the angolan shield, Congo craton. In: Siegesmund, S., Oyhantçabal, P., Basei, M.A.S., Oriolo, S. (Eds.), Geology of Southwest Gondwana. Regional Geology Reviews, Springer, Heidelberg, pp. 217–239.
Jung, S., Kröner, A., Kröner, S., 2007. A~ 700 ma Sm–Nd garnet–whole rock age from the granulite facies central kaoko zone (Namibia): evidence for a cryptic high-grade polymetamorphic history? Lithos 97 (3–4), 247–270.
Jung, S., Masberg, P., Mihm, D., Hoernes, S., 2009. Partial melting of diverse crustal sources—constraints from Sr–Nd–O isotope compositions of quartz diorite–granodiorite–leucogranite associations (Kaoko Belt, Namibia). Lithos 111 (3–4), 236–251.
Jung, S., Mezger, K., Nebel, O., Kooijman, E., Berndt, J., Hauff, F., Münker, C., 2012. Origin of meso-proterozoic post-collisional leucogranite suites (kaokoveld, Namibia): constraints from geochronology and nd, sr, hf, and pb isotopes. Contrib. Miner. Petrol. 163, 1–17.
Jung, S., Brandt, S., Nebel, O., Hellebrand, E., Seth, B., Jung, C., 2014. The P-t–t paths of high-grade gneisses, Kaoko Belt, Namibia: constraints from mineral data, U–Pb allanite and monazite and Sm–Nd/Lu–Hf garnet ages and garnet ion probe data. Gondw. Res. 25 (2), 775–796.
Kleinhanns, I.C., Fullgraf, T., Wilsky, F., Nolte, N., Fliegel, D., Klemd, R., Hansen, B.T., 2015. U-pb zircon ages and (isotope) geochemical signatures of the kamanjab inlier (NW Namibia): constraints on palaeoproterozoic crustal evolution along the southern Congo craton. Special Publications of the Geological Society of London 389 (1), 165–195.
Koester, E., Porcher, C.C., Pimentel, M.M., Fernandes, L.A.D., Vignol-Lelarge, M.L., Oliveira, L.D., Ramos, R.C., 2016. Further evidence of 777 ma subduction-related continental arc magmatism in eastern Dom Feliciano Belt, southern Brazil: the Chácara das pedras orthogneiss. J. s. Am. Earth Sci. 68, 155–166.
Konopásek, J., Kröner, S., Kitt, S.L., Passchier, C.W., Kröner, A., 2005. Oblique collision and evolution of large-scale transcurrent shear zones in the kaoko belt. NW Namibia. Precambrian Research 136 (2), 139–157.
Konopásek, J., Košler, J., Tajčmanová, L., Ulrich, S., Kitt, S.L., 2008. Neoproterozoic igneous complex emplaced along major tectonic boundary in the Kaoko Belt (NW Namibia): ion probe and LA-ICP-MS dating of magmatic and metamorphic zircons. J. Geol. Soc. Lond. 165 (1), 153–165.
Konopásek, J., Košler, J., Sláma, J., Janoušek, V., 2014. Timing and sources of pre-collisional neoproterozoic sedimentation along the SW margin of the Congo craton (Kaoko Belt, NW Namibia). Gondw. Res. 26, 386–401.
Konopásek, J., Sláma, J., Košler, J., 2016. Linking the basement geology along the Africa-South America coasts in the South Atlantic. Precambr. Res. 280, 221–230.
Konopásek, J., Hoffmann, K.-H., Sláma, J., Košler, J., 2017. The onset of flysch sedimentation in the Kaoko Belt (NW Namibia) – implications for the pre-collisional evolution of the kaoko-Dom Feliciano-Gariep orogen. Precambr. Res. 298, 220–234.
Konopásek, J., Janoušek, V., Oyhantçabal, P., Sláma, J., Ulrich, S., 2018. Did the circumrodinia subduction trigger the neoproterozoic rifting along the Congo-Kalahari craton margin? Int. J. Earth Sci. 107 (5), 1859–1894.
Konopásek, J., Cavalcante, C., Fossen, H., Janoušek, V., 2020. Adamastor – an ocean that never existed? Earth Sci. Rev. https://doi.org/10.1016/j.earscirev.2020.103201.
Kröner, S., Konopásek, J., Kröner, A., Passchier, C.W., Poller, U., Wingate, M.W.D., Hofmann, K.H., 2004. U-pb and pb-pb zircon ages for metamorphic rocks in the Kaoko Belt of northwestern Namibia: a palaeo- to mesoproterozoic basement reworked during the Pan-african orogeny. S. Afr. J. Geol. 107, 455–476.
Kröner, A., Rojas-Agramonte, Y., 2017. Mesoproterozoic (Grenville-age) granitoids and supracrustal rocks in kaokoland, northwestern Namibia. Precambr. Res. 298, 572–592.
Kröner, A., Rojas-Agramonte, Y., Hegner, E., Hoffmann, K.-H., Wingate, M.T.D., 2010. SHRIMP zircon dating and nd isotopic systematics of palaeoproterozoic migmatitic orthogneisses in the epupa metamorphic complex of northwestern Namibia. Precambr. Res. 183, 50–69.
Kröner, A., Rojas-Agramonte, Y., Wong, J., Wilde, S.A., 2015. Zircon reconnaissance dating of proterozoic gneisses along the Kunene River of northwestern Namibia. Tectonophysics 662, 125–139.
Lara, P., Oyhantçabal, P., Dadd, K., 2017. Post-collisional, late neoproterozoic, high-Ba-sr granitic magmatism from the Dom Feliciano Belt and its cratonic foreland, Uruguay: petrography, geochemistry, geochronology, and tectonic implications. Lithos 277, 178–198.
Lara, P., Oyhantçabal, P., Belousova, E., 2020. Two distinct crustal sources for late neoproterozoic granitic magmatism across the sierra ballena Shear zone, Dom Feliciano Belt, Uruguay: whole-rock geochemistry, zircon geochronology and sr-nd-hf isotope evidence. Precambr. Res. 341, 105625.
Lara, P., Oyhantçabal, P., Belousova, E., Hueck, M., 2021. Source diversity of late neoproterozoic granitoid magmatism across an orogen-scale lineament in southern Brazil and Uruguay: whole-rock geochemistry, zircon geochronology and sr-nd-hf isotope evidence. J. s. Am. Earth Sci. 112, 103597.
Laurent, O., Martin, H., Moyen, J.F., Doucelance, R., 2014. The diversity and evolution of late-archean granitoids: evidence for the onset of "modern-style" plate tectonics between 3.0 and 2.5 ga. Lithos 205, 208–235.
Lenz, C., Fernandes, L.A.D., McNaughton, N.J., Porcher, C.C., Masquelin, H., 2011. U-pb SHRIMP ages for the cerro Bori orthogneisses, Dom Feliciano Belt in Uruguay: evidences of a ~800 ma magmatic and a ~650 ma metamorphic event. Precambr. Res. 185, 149–163.

Liew, T.C., Hofmann, A.W., 1988. Precambrian crustal components, plutonic associations, plate environment of the hercynian Fold Belt of central Europe: indications from a nd and sr isotopic study. Contrib. Miner. Petrol. 98, 129–138.
Lino, L.M., Quiroz-Valle, F.R., Basei, M.A.S., Vlach, S.R.F., Hueck, M., Willbold, M., Citroni, S.B., Lemo-Santos, D.V., 2023. Petrogenesis and tectonic significance of two bimodal volcanic stages from the Ediacaran Campo Alegre-Corupá Basin (Brazil): record of metacratonization during the consolidation of Western Gondwana. Precambr. Res. 106950.
Lopes, A.P., 2008. Geologia do Complexo Camboriú, SC. Igc-USP. PhD Thesis.
Ludwig, K.R., 2008. Isoplot 3.70. A geochronological toolkit for Microsoft Excel. Berkeley Geochronology Center Special Publications, Berkeley.
Masberg, P., Mihm, D., Jung, S., 2005. Major and trace element and isotopic (sr, nd, O) constraints for Pan-african crustally contaminated grey granite gneisses from the southern kaoko belt, Namibia. Lithos 84 (1–2), 25–50.
Masquelin, H., Fernandes, L.A.D., Lenz, C., Porcher, C.C., McNaughton, N.J., 2012. The cerro Olivo complex: a pre-collisional elationshipc magmatic arc in eastern Uruguay. International Geological Review 54, 1161–1183.
Matté, V., Sommer, C.A., Lima, E.F., Philipp, R.P., Basei, M.A.S., 2016. Post-collisional Ediacaran volcanism in oriental ramada plateau, southern Brazil. J. s. Am. Earth Sci. 71, 201–222.
Matzel, J.E.P., Bowring, S.A., Miller, R.B., 2006. Time scales of pluton construction at differing crustal levels: examples from the Mount Stuart and Tenpeak intrusions, north cascades, Washington. Geol. Soc. Am. Bull. 118 (11/12), 1412–1430.
Middlemost, E.A., 1994. Naming materials in the magma/igneous rock system. Earth Sci. Rev. 37 (3–4), 215–224.
Miller, J.S., Matzel, J.E.P., Miller, C.F., Burgess, S., Miller, R.B., 2007. Zircon growth and recycling during the assembly of large, composite arc plutons. J. Volcanol. Geoth. Res. 167, 282–299.
Miller, C.F., McDowell, S.M., Mapes, R.W., 2003. Hot and cold granites? implications of zircon saturation temperatures and preservation of inheritance. Geology 31 (6), 529–532.
Moraes, L.V., Florisbal, L.M., de Assis Janasi, V., Bitencourt, M.F., Martins, L., Heaman, L.M., Stern, R., 2023. Elemental and isotopic (sr-nd-O) geochemistry and upb zircon geochronology of late-stage, post-collisional, shallow-level magmatism in the Dom Feliciano Belt northern sector. Lithos 442, 107057.
Moyen, J.F., Laurent, O., Chelle-Michou, C., Couzinié, S., Vanderhaeghe, O., Zeh, A., Gardien, V., 2017. Collision vs. subduction-related magmatism: two contrasting ways of granite formation and implications for crustal growth. Lithos 277, 154–177.
Moyen, J.F., Janoušek, V., Laurent, O., Bachmann, O., Jacob, J.B., Farina, F., Villaros, A., 2021. Crustal melting vs. fractionation of basaltic magmas: Part 1, granites and paradigms. Lithos 402, 106291.
Ohta, T., Arai, H., 2007. Statistical empirical index of chemical weathering in igneous rocks: A new tool for evaluating the degree of weathering. Chem. Geol. 240 (3–4), 280–297.
Oriolo, S., Oyhantçabal, P., Wemmer, K., Heidelbach, F., Pfänder, J., Basei, M.A.S., Hueck, M., Hannich, F., Sperner, B., Siegesmund, S., 2016a. Shear zone evolution and timing of deformation in the neoproterozoic transpressional Dom Feliciano Belt, Uruguay. J. Struct. Geol. 92, 59–78.
Oriolo, S., Oyhantçabal, P., Basei, M.A.S., Wemmer, K., Siegesmund, S., 2016b. The Nico pérez terrane (Uruguay): from archean crustal growth and connections with the Congo craton to late neoproterozoic accretion to the río de la Plata craton. Precambr. Res. 280, 147–160.
Oriolo, S., Oyhantçabal, P., Wemmer, K., Siegesmund, S., 2017. Contemporaneous assembly of Western Gondwana and final rodinia break-up: implications for the supercontinent cycle. Geosci. Front. 8 (6), 1431–1445.
Oriolo, S., Hueck, M., Oyhantçabal, P., Goscombe, B., Wemmer, K., Siegesmund, S., 2018. Shear zones in brasiliano-Pan-african belts and their role in the amalgamation and break-up of Southwest Gondwana. In: Siegesmund, S., Oyhantçabal, P., Basei, M. A.S., Oriolo, S. (Eds.), Geology of Southwest Gondwana. Regional Geology Reviews, Springer, Heidelberg, pp. 593–613.
Oyhantçabal, P., Siegesmund, S., Wemmer, K., Presnyakov, S., Layer, P., 2009. Geochronological constraints on the evolution of the southern Dom Feliciano Belt (Uruguay). J. Geol. Soc. Lond. 166, 1075–1084.
Oyhantçabal, P., Siegesmund, S., Wemmer, K., Passchier, C.W., 2011. The transpressional connection between Dom Feliciano and Kaoko belts at 580–550 ma. Int. J. Earth Sci. 100, 379–390.
Oyhantçabal, P., Cingolani, C.A., Wemmer, K., Siegesmund, S., 2018. The río de la Plata craton of Argentina and Uruguay. In: Siegesmund, S., Oyhantçabal, P., Basei, M.A.S., Oriolo, S. (Eds.), Geology of Southwest Gondwana. Regional Geology Reviews, Springer, Heidelberg, pp. 89–105.
Passarelli, C.R., Basei, M.A.S., Siga Jr, O., Mc Reath, I., Campos Neto, M.C., 2010. Deformation and geochronology of syntectonic granitoids emplaced in the Major Gercino Shear zone, southeastern south America. Gondw. Res. 17, 688–703.
Passarelli, C.R., McReath, I., Basei, M.A.S., Siga Jr, O., Campos Neto, M.C., 2011. Heterogeneity in syntectonic granitoids emplaced in a major shear zone, southern Brazil. J. s. Am. Earth Sci. 32, 369–378.
Passchier, C.W., Trouw, R.A., Goscombe, B., Gray, D., Kröner, A., 2007. Intrusion mechanisms in a turbidite sequence: the voetspoor and doros plutons in NW Namibia. J. Struct. Geol. 29 (3), 481–496.
Passchier, C., Trouw, R., da Silva Schmitt, R., 2016. How to make a transverse triple junction—New evidence for the assemblage of Gondwana along the kaoko-Damara belts. Namibia. Geology 44 (10), 843–846.
Peccerillo, A., Taylor, S.R., 1976. Geochemistry of eocene calc-alkaline volcanic rocks from the Kastamonu area, northern Turkey. Contrib. Miner. Petrol. 58, 63–81.
Percival, J.J., Konopásek, J., Anczkiewicz, R., Ganerød, M., Sláma, J., de Campos, R.S., Bitencourt, M.F., 2022. Tectono-Metamorphic Evolution of the Northern Dom Feliciano Belt Foreland, Santa Catarina, Brazil: Implications for Models of Subduction-Driven Orogenesis. Tectonics 41(2), e2021TC007014.
Percival, J.J., Konopásek, J., Eiesland, R., Sláma, J., de Campos, R.S., Battisti, M.A., Bitencourt, M.F., 2021. Pre-orogenic connection of the foreland domains of the kaoko-Dom feliciano–Gariep orogenic system. Precambr. Res. 354, 106060.
Peruchi, F.M., Florisbal, L.M., Bitencourt, M.F., Padilha, D.F., Nardi, L.V.S., 2021. Ediacaran post-collisional K-rich granitic magmatism within the Major Gercino Shear zone, southern Brazil: an example of prolonged magmatism and differentiation under active transcurrent tectonism. Lithos 402, 106341.
Perugini, D., Poli, G., 2012. The mixing of magmas in plutonic and volcanic environments: analogies and differences. Lithos 153, 261–277.
Philipp, R.P., Pimentel, M.M., Chemale Jr., F., 2016. Tectonic evolution of the Dom Feliciano Belt in southern Brazil: geological relationships and U-pb geochronology. Braz. J. Geol. 46 (1), 83–104.
Ramos, R.C., Edinei, K., Triboli, V.D., Cristine, P.C., Neri, G.J., Luiz, S.R., 2018. Insights on the evolution of the Arroio Grande ophiolite (Dom Feliciano belt, Brazil) from rb-sr and SHRIMP U-pb isotopic geochemistry. J. s. Am. Earth Sci. 86, 38–53.
Ramos, R.C., Koester, E., Vieira, D.T., 2020. Sm–Nd systematics of metaultramafic-mafic rocks from the Arroio Grande ophiolite (Brazil): insights on the evolution of the south Adamastor paleo-ocean. Geosci. Front. https://doi.org/10.1016/j.gsf.2020.02.013.
Rapela, C.W., Fanning, C.M., Casquet, C., Pankhurst, R.J., Spalletti, L., Poiré, D., Baldo, E.G., 2011. The río de la Plata craton and the adjoining Pan-african/brasiliano terranes: their origins and incorporation into south-west Gondwana. Gondw. Res. 20, 673–690.
Rudnick, R., Gao, S., 2003. Composition of the continental crust. In: Rudnick, R.L. (Ed.), The Crust. In: Holland, H.D., Turekian, K.K. (Eds.), Treatise on Geochemistry, vol. 3, Elsevier–Pergamon, Oxford, 1–64.
Saalmann, K., Gerdes, A., Lahaye, Y., Hartmann, L.A., Remus, M.V.D., Läufer, A., 2011. Multiple accretion at the eastern margin of the rio de la Plata craton: the prolonged brasiliano orogeny in southernmost Brazil. Int. J. Earth Sci. 100, 355–378.
Saint Blanquat, M., Horsman, E., Habert, G., Morgan, S., Vanderhaeghe, O., Law, R., Tikoff, B., 2011. Multiscale magmatic cyclicity, duration of pluton construction, and the paradoxicelationshiphip between tectonism and plutonism in continental arcs. Tectonophysics 500, 20–33.
Schaltegger, U., Brack, P.B., Ovtcharova, M., Peytcheva, I., Schoene, B., Stracke, A., Bargossi, G.M., 2009. Zircon U, pb, th, and hf isotopes record up to 700 kyrs of magma fractionation and crystallization in a composite pluton (adamello batholith, N Italy). Earth and Planetary Sciences Letters 286, 208–218.
Schmitt, R.S., Trouw, R.A., Passchier, C.W., Medeiros, S.R., Armstrong, R., 2012. 530 ma syntectonic syenites and granites in NW Namibia—Their relation with collision along the junction of the Damara and kaoko belts. Gondw. Res. 21 (2–3), 362–377.
Seth, B., Kröner, A., Mezger, K., Nemchin, A.A., Pidgeon, R.T., Okrusch, M., 1998. Archean to neoproterozoic magmatic events in the Kaoko Belt of NW Namibia and their geodynamic significance. Precambr. Res. 92, 341–363.
Seth, B., Okrusch, M., Wilde, M., Hoffmann, K.H., 2000. The voetspoor intrusion, southern kaoko zone, Namibia: mineralogical, geochemical and isotopic constraints for the origin of a syenitic magma. Communicationsof the Geological Survey of Namibia 12, 125–137.
Seth, B., Jung, S., Hoernes, S., 2002. Isotope constraints on the origin of Pan-african granitoid rocks in the kaoko belt, NW Namibia. S. Afr. J. Geol. 105 (2), 179–192.
Seth, B., Jung, S., Gruner, B., 2008. Deciphering polymetamorphic episodes in high-grade metamorphic orogens: constraints from PbSL, Sm/Nd and Lu/Hf garnet dating of low-to high-grade metasedimentary rocks from the kaoko belt (Namibia). Lithos 104 (1–4), 131–146.
Shand, S.J., 1943. Eruptive rocks: their genesis, composition, classification, and their relation to ore deposits with a chaper on meteorites. J. Wiley & Sons.
Silva, L.C., Armstrong, R., Pimentel, M.M., Scandolara, J., Ramgrab, G., Wildner, W., Angelim, L.A.A., Vasconcelos, A.M., Rizzoto, G., Quadros, M.L.E.S., Sander, A., Rosa, A.L.Z., 2002. Reavaliação da evolução geológica em terrenos pré-cambrianos brasileiros com base em novos dados U-pb SHRIMP, Parte III: províncias Borborema, Mantiqueira meridional e Rio Negro-Juruena. Revista Brasileira De Geociências 32 (4), 529–544.
Silva Lara, H., Siegesmund, S., Oriolo, S., Hueck, M., Wemmer, K., Basei, M.A.S., Oyhantçabal, P., 2022. Reassessing the polyphase neoproterozoic evolution of the Punta del Este terrane, Dom Feliciano Belt. Uruguay. International Journal of Earth Sciences 111 (7), 2283–2316.
Silva, L.C., McNaughton, N.J., Hartmann, L.A., Fletcher, I.R., 2003. Contrasting zircon growth patterns in neoproterozoic granites of southern Brazil revealed by SHRIMP U-pb analyses and SEM imaging: consequences for the discrimination of emplacement and inheritance ages. In: IV South American Symposium on Isotope Geology. Salvador, Bahia, Brazil. Short Papers, pp. 687–690.
Silva, L.C., McNaughton, N.J., Fletcher, I.R., 2005. Reassesment on complex zircon populations from neoproterozoic granites in Brazil, through SEM imaging and SHRIMP analysis: consequences for discrimination of emplacement and inherited ages. Lithos 82 (3–4), 503–525.
Sommer, C.A., de Lima, E.F., Nardi, L.V.S., Figueiredo, A.M.G., Pierosan, R., 2005. Potassic and low-and high-ti mildly alkaline volcanism in the neoproterozoic ramada plateau, southernmost Brazil. J. s. Am. Earth Sci. 18 (3–4), 237–254.
Sun, S.S., McDonough, W.F., 1989. Chemical and isotopic systematics of oceanic basalts: implications for mantle composition and processes. Geol. Soc. Lond. Spec. Publ. 42 (1), 313–345.
Taylor, S.R., McLennan, S.M., 1985. The continental crust: its composition and evolution. Blackwell Scientific Publication, Oxford, p. 312.

Ulrich, S., Konopásek, J., Jeřábek, P., Tajčmanová, L., 2011. Transposition of structures in the neoproterozoic Kaoko Belt (NW Namibia) and their absolute timing. Int. J. Earth Sci. 100 (2–3), 415–429.
Vermeesch, P., 2012. On the visualization of detrital age distributions. Chem. Geol. 312–313, 190–194.
Villaros, A., Buick, I.S., Stevens, G., 2012. Isotopic variations in S-type granites: an inheritance from a heterogeneous source? Contrib. Miner. Petrol. 163 (2), 243–257.
Will, T.M., Okrusch, M., Gruner, B.B., 2004. Barrovian and buchan type metamorphism in the Pan-african kaoko belt, Namibia: implications for its geotectonic position within the framework of Western Gondwana. S. Afr. J. Geol. 107 (3), 431–454.
Will, T.M., Gaucher, C., Ling, X.X., Li, X.H., Li, Q.L., Frimmel, H.E., 2019. Neoproterozoic magmatic and metamorphic events in the cuchilla dionisio terrane, Uruguay, and possible correlations across the South Atlantic. Precambr. Res. 320, 303–322.
Will, T.M., Höhn, S., Frimmel, H.E., Gaucher, C., le Roux, P.J., Macey, P.H., 2020. Petrological, geochemical and isotopic data of neoproterozoic rock units from Uruguay and South Africa: Correlation of basement terranes across the South Atlantic. Gondw. Res. 80, 12–32.